TUMOR-OSTEOCYTE INTERACTIONS UNDER FLUID FLOW STIMULATION

A Thesis

Submitted to the Faculty

of

Purdue University

by

Aydin Jalali

In Partial Fulfillment of the

Requirements for the Degree

of

Master of Science in Biomedical Engineering

August 2018

Purdue University

Indianapolis, Indiana

THE PURDUE UNIVERSITY GRADUATE SCHOOL
STATEMENT OF COMMITTEE APPROVAL

Dr. Hiroki Yokota, Chair

Department of Biomedical Engineering

Dr. Julie Ji

Department of Biomedical Engineering

Dr. Sungsoo Na

Department of Biomedical Engineering

Approved by:

Dr. Edward Berbari

Head of the Graduate Program

ACKNOWLEDGMENTS

First of all, I would like to thank my advisor Dr. Hiroki Yokota for his consistent support and mentorship. Without his patience, persistent help, and encouragement this thesis would not have been possible. I would like to thank my committee members, Dr. Julie Ji and Dr. Sungsoo Na, for their support, suggestions, and encouragement.

I would like to express my deepest thanks and sincere appreciation to Dr. Andy Chen for his excellent guidance, brilliant notions to initiate and develop this study, teaching me many techniques, and his consistent support. I would also like to thank Yao Fan, for her selfless support, and her tremendous contributions to this study, such as performing western blot and 3D tumor spheroid assays, tumor induction in mice, and helping me in conducting many experiments. Thanks go to all my colleagues in Dr. Yokota's lab past and present, including, Dr. Shengzhi Liu, Luqi Wang, Yue Wang, Rika Kondo, Chie Deguchi, and Azusa Ishizaki. Special thanks go to Sherry Clemens for helping me with all the administrative work.

I would like to give my most profound appreciation to my family, and friends who have supported me through all the hardships and have been my confidant and warmth of my heart.

Finally, I would like to thank God, who no hand and tongue are capable of fulfilling the obligations of thanks to him.

TABLE OF CONTENTS

Page

Page

LIST OF FIGURES

Figure Page

LIST OF ABBREVIATIONS

BMD	bone morphogenetic proteins
BMP	bone morphogenetic protein
LPS	lipopolysaccharide
MMP	matrix metalloproteinase
CM	conditioned medium
COX2	cyclooxygenase 2
EMT	epithelial-mesenchymal transition
FBS	fetal bovine serum
FCS	fetal calf serum
FGF	fibroblast growth factor
FF	fluid flow
FFCM	fluid flow-treated conditioned medium
FRET	fluorescence resonance energy transfer
IGF	insulin-like growth factor
LOX	lysyl oxidase
MEM	minimum essential medium
MET	mesenchymal-epithelial transition
MMP	matrix metalloproteinase
NO	nitric oxide
RANK	receptor activated nuclear factor-κB
OPN	osteopontin
OPG	osteoprotegerin
PTHrP	parathyroid hormone-related protein
PBS	phosphate buffered saline

PDGF	platelet-derived growth factor
PGE2	prostaglandin E2
Runx2	runt-related transcription factor 2
TRAP	tartrate-resistant acid phosphatase
TGF	transforming growth factor
TNF-α	tumor necrosis factor-alpha

ABSTRACT

Jalali, Aydin M.S.B.M.E., Purdue University, August 2018. Tumor-Osteocyte Interactions Under Fluid Flow Stimulation. Major Professor: Hiroki Yokota.

Bone is one of the most common sites for breast cancer metastasis. Osteocytes compose approximately 90% of the cell population in bone matrix. Osteocytes are very sensitive to mechanical stimulation, and physical activities play an essential role in maintaining bone's health. Mechanical stimulation can alter the gene expression profile in osteocytes. However, little is known about the effects of mechanical stimulation on tumor-bone interactions. In this thesis, this question has been addressed: Does applying mechanical stimulation to osteocytes change tumor-osteocytes interactions? The hypothesis is that mechanical stimulation can change osteocytes secreting signals and contribute to higher proliferation and migration of tumor cells.

In this thesis, fluid flow-driven shear stress has been used as the mechanical stimulator for osteocytes, and the interactions of tumor-osteocytes, with and without mechanical stimulation has been investigated. Monolayer cultures and 3D spheroids of breast cancer cells, including TMD and 4T1 cells were cultured in the conditioned medium (CM) isolated from MLO-A5 osteocytes, and fluid flow-treated conditioned medium (FFCM), and their migratory behavior, proliferation, and protein expression have been evaluated. The results showed that in response to MLO-A5 FFCM, tumor cells behave differently in Src expression, proliferation, and migration compared to MLO-A5 CM. As opposed to MLO-A5 CM, FFCM promoted migration, reduced proliferation, and upregulated Src expression in tumor cells. Moreover, by plasmid and siRNA transfection it has been shown that Src is upstream of Snail and their upregulation is causing epithelial-mesenchymal transition(EMT) responses in tumor cells.

Furthermore, ELISA concentration assessment showed the involvement of TGF-β in Src upregulation.

An *in vivo* study using seventeen mice was conducted to investigate the effect of mechanical stimulation on clinical conditions. Compressive loads were applied to tibia after intratibial injection of 4T1.2 cells. The results suggested that direct mechanical stimulation of metastasized bone, might not be advantageous, and cause more damage. Furthermore, the results indicated that direct mechanical loading can make the knee joint more fragile. This research showed mechanical stimulation can cause tumor cells to behave more migratory in bone microenvironment, and demonstrated its crucial role in tumor-osteocytes interactions.

1. INTRODUCTION

1.1 Breast Cancer and Metastasis

Breast cancer has the second highest fatality rate among cancers in women [1]. Despite the advances in the recent years, metastatic breast cancer can hardly be cured in many cases because of its intrinsic heterogeneity and resistance to existing drugs. The studies have shown that the metastatic cells carry specific biological attributes of primary tumors in addition to distinct characteristics such as intensified motility, invasiveness, survival, and resistance to chemotherapy [2]. In the late-stage breast cancer, several tissues are usually affected by the tumor including bone, liver, and lung [3]. The metastasis site may depend on varying factors including complementary adhesive contacts, tumor cells and the stroma molecular interactions and, vascular flow pattern at the primary tumor site.

The primary tumor cells may experience a series of biological steps to develop metastatic cells. This process is called a metastatic cascade that includes invasion, migration, and colonization. Invasion is the first step in this process that happens with changes in cell-cell and cell-matrix adhesion. Invasion is recognizable with the switch in cadherin family expression, and extracellular matrix (ECM) degradation [4]. In the next step, tumor cells migrate to distant organs. Studies have shown that there is two main processes for tumor cells migration, including single-cell and collective-cell migration. EMT has shown to be essential for mesenchymal-cell migration. In addition, Rho GTPases seem to be an important factor in amoeboid single-cell migration. EMT and Rho GTPases increase matrix metalloproteinase (MMP) activation, which causes more ECM degradation and more invasive stage. During the EMT process, tumor cells go through multiple changes that lead to invasion including downregulation of epithelial-associated genes and amplification of mesenchymal-genes expression,

changes in cells cytoskeleton, and loosen cell-cell contact. By EMT, some tumor cells gain the ability to invade the basement membrane and surrounding stroma, and subsequently, they invade blood or lymphatic vessels. Several mechanisms have been shown that can promote and control EMT in cancer cells, including Wnt signaling, Notch signaling, and other molecules including tumor necrosis factor-alpha (TNF-α), and Src.

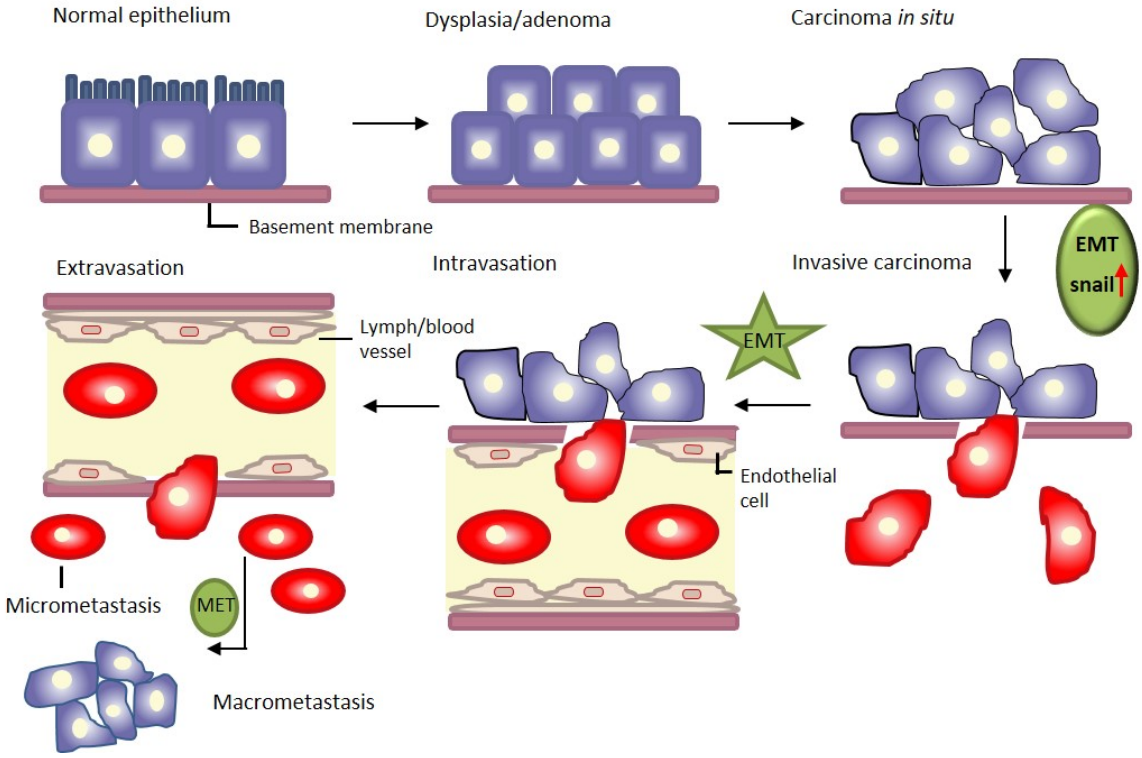

Fig. 1.1.: EMT process [5].

Studies have shown that in 50% of breast cancer patients the Wnt signaling is activated, and its activation is associated with declined overall survival [6]. In most cases, the canonical Wnt ligands and receptors are overexpressed, while the secreted antagonists are silenced. Activation of Wnt/β-catenin pathway leads to Snail expression. Subsequently, the process causes E-cadherin downregulation and vimentin upregulation. While activation of Wnt signaling is linked to EMT, studies have shown that

β-catenin expression alone, cannot cause EMT [7]. In addition, osteocytes activate Wnt signaling through Lrp5/Lrp6 receptors, and cause osteogenic genes in bone-forming osteoblasts . Lrp5 is a co-receptor known in Frizzled protein family members and plays an important role in adjusting Wnt signaling and load-driven-bone formation [8]. Based on Rabbani et al. report, Lrp5 knockdown caused MET-like responses in prostate cancer cells such as decreased migration, invasion, and increased cell proliferation [9].

Notch signaling is another modulator of Snail expression. Notch signaling regulates Snail expression through two mechanisms: direct transcriptional activation of Snail, and the indirect mechanism by lysyl oxidase (LOX). Upregulation of LOX leads to Snail upregulation, which eventually activates EMT program and induces migratory and invasive cancer [10, 11].

TNF-α is a cytokine, which is involved in various processes in the body, such as cellular homeostasis, inflammation, and tumor progression. Studies have shown that TNF-α can block E-cadherin expression while promoting MMP9 expression. The underlying mechanism is not clear. However, upregulation of Twist-1 has been hypothesized to be one of the associated factors. In breast cancer patients, upregulation of TNF-α is one of the indicators of invasive cancer [12, 13].

Src is a non-receptor tyrosine kinase. Src is one of the critical signaling molecules in tumorigenesis and is involved in other cell activities, including proliferation, growth, angiogenesis, motility, adhesion, and survival [14]. Upregulation of Src in tumor cells is a sign of excessive growth, and metastasis. Studies have shown that Src interacts with and mediates signaling from multiple cell surface receptors associated with angiogenesis, and tumor proliferation such as vascular endothelial growth factor receptor, epidermal growth factor receptor, etc [15, 16]. Based on Saad et al. report, Src elevation is associated with increased bone metastasis and cancer cell growth in bone metastases [17]. Moreover, Src upregulation can stimulate PTH-rP production.

For the purpose of this study, two cancer cell lines were used: TMD and 4T1.2 cell lines. TMD tumor cells are a clone of MDA-MB-231 cells. These cells have

been harvested from a mammary tumor after injecting MDA-MB-231 cells into the mammary fat of NOD/SCHID mouse. MDA-MB-231 cell line is an epithelial, human breast cancer cell line, which is extremely invasive and aggressive. This cell line is triple negative, without detectable expression of estrogen receptor (ER), progesterone receptor (PR), and human epidermal growth factor receptor 2 (HER2) [18]. 4T1.2 cell line is a clone of 4T1 cells. 4T1 cell line is commonly used in medical research to mimic the stage IV human breast cancer in the animal model. After injecting 4T1 cells into the mammary pad and creation of spontaneous mammary tumor, 4T1.2 cells were derived from the metastasized bone [3].

1.2 Bone Structure and Remodeling

Bone is comprised of both mineral and organic components. Inorganic hydroxyapatite (65%), organic collagen (10%), and water (25%) are the three main components which create the bone tissue. Among the cartilage, bone is one of the main parts in the skeletal body system [19]. The skeletal system is mainly responsible to provide structural support for softer tissues in the body such as lungs, heart, brain, etc. The other key functionality of the bone is its role in the body movement by being an attachment and support site for the muscles. Moreover, bone is the main reservoir of calcium and phosphorus in the body.

There are two primary mechanisms for bone formation; intramembranous ossification, and endochondral ossification [19]. In intramembranous ossification, the embryonic tissue or mesenchyme is differentiated into osteoblasts which will develop the flat bones. In endochondral ossification, first the cartilage model of the bone is created, and the bone is replaced subsequently. Most of the long bones in the body are made through the endochondral ossification. The cartilage model of the bone is created by condensation of mesenchymal cells, which are differentiated to chondrocytes afterward [20]. The chondrocytes will secrete different components to form the cartilage ECM. Furthermore, the chondrocytes in the center of the model, will grow and

initiate the calcification process, which leads to their differentiation into osteoblasts. This process causes the transformation of perichondrium of surrounding cartilage to the periosteum. As osteoclasts resorb the remaining cartilage, and osteoblasts generate osteoid forming trabeculae to form the bone structure, the diaphysis initiates to elongate and creates the medullary cavity. By entering vessels to the ends of the cartilage model or epiphysis, the secondary ossification centers are formed. Diaphysis and epiphysis are separated by the growth plate. Growth plate consists of cartilage, and bone can continue to grow through hypertrophy of the chondrocytes within the growth plate. Chondrocytes hypertrophy leads to matrix deposition, which allows osteoblasts to promote matrix and minerals deposition [19].

Bone remodeling is an important mechanism which able the bone to bear tremendous loads in everyday life. Osteoclasts and osteoblasts are the main components of this process, and their population plays an important role in adjusting it. The osteoclasts differentiation depends mainly on RANKL/RANK/OPG pathway. The macrophage colony-stimulating factor (M-CSF), interacts with c-fms which leads to monocyte progenitor proliferation and expression of receptor activator of nuclear factor-kB (RANK) [21]. The osteoblasts express RANK ligand (RANKL), which stimulates the osteoclast differentiation. By RANKL interaction with RANK, the NF-kB signaling is activated, which causes the mononuclear osteoclasts to express tartrate-resistant acid phosphatase (TRAP) [19]. While osteoblast can stimulate and cause osteoclast differentiation by producing RANKL, osteonectin, osteopontin, and osteocalcin, it can inhibit osteoclast differentiation by limiting receptor osteoprotegerin (OPG) [22].

Osteoblasts are derived from two progenitor cells, neural and mesodermal. Briefly, the runt-related transcription factor 2 (Runx2) modulate gene expressions which encode osteocalcin, RANKL, VEGF, dentin matrix protein 1 (DMP1) and sclerostin, that are responsible for stimulating progenitor cell differentiation into osteoblast lineage [23]. Moreover, growth factors such as fibroblast growth factor (FGF) and insulin-like growth factor (IGF), angiogenic factors including endothelin-1, hormones

like prostaglandin agonists and PTH, and bone morphogenetic proteins (BMPs), all regulate osteoblast differentiation [24].

For the bone remodeling, osteoclasts secret hydrolytic enzymes which can degrade collagen in the matrix. These enzymes include metalloproteases and cathepsin K, such as lysosomal hydrolases that degrade the matrix in 2-4 weeks. The degraded mineral components are removed by the circulation, which leads to the formation of an empty space called resorption pit [19]. After resorption, osteoclasts go through apoptosis and are replaced by osteoblasts. Eventually, osteoblasts create the new matrix in 4-6 months. At the end of their life cycle, osteoblasts go through a terminal differentiation and transform to osteocytes inside the mineralized matrix. The osteocytes maintain the bone microenvironment balance, control phosphate metabolism, and adjust bone formation by expressing molecules including FGF 23, DMP1, and sclerostin [25].

1.3 Bone Metastasis and Bone Destruction

Bone has been the most common site for breast cancer metastasis [3]. Usually, bone metastasis leads to spinal cord compression, extreme pain, hypercalcemia, and bone fractures. The tradition of chemotherapy has shown to be not effective despite alleviating the metastasis symptoms for a short period [26]. By expressing chemokines receptors, tumor cells gain the ability to migrate to specific organs. In addition, bone matrix is an excellent reservoir for different growth factors such as platelet-derived growth factors (PDGFs), BMPs , FGFs, and transforming growth factor α and β (TGF-α and β) [27].

During osteoclastic bone degradation and resorption, most of these growth factors are released into the marrow. This process can create a chemotactic and attractive site for tumor cells to grow. Furthermore, bone marrow-derived hematopoietic cells have the ability to provide premetastatic niche which can facilitate targeted colonization [27]. Many studies have shown how invading of breast cancer cells to the bone can cause bone degradation in a process called viscous cycle [27]. There are

four main components that are involved in the vicious cycle which include osteoclasts, osteoblasts, mineralized bone matrix, and tumor cells. Due to the production of different growth factors in the bone microenvironment by tumor cells such as parathyroid hormone-related protein (PTHrP), the protein expression in the bone cells change [28]. Notably, the RANKL protein expression is upregulated and OPG expression is downregulated. These changes lead to more osteoclasts activity and bone degradation [29]. In addition, cytokines such as IL-6, IL-8, and IL-11 which are expressed by breast cancer cells can boost the osteoclasts activity. One of the key factors in bone metastasis osteolysis process is TGF-β [30]. The studies have shown that TGF-β can active Smad-dependent and Smad-independent signal pathways which can cause pre-osteolytic factors such as PTHrP to be expressed [27].

1.4 Role of Osteocytes in Bone Metastasis

Over 90% of the cells in a mineralized section of the bone is composed of osteocytes which are derived from osteoblasts [31]. Osteocytes play a vital role in regulating bone homeostasis by adjusting bone formation and resorption in different conditions. Studies have shown that production of metastatic-mediate factors including osteopontin (OPN) and RANKL by osteocytes are upregulated in breast cancer bone metastasis and accelerate the bone resorption. In addition, osteocytes can affect osteoclasts formation by secreting factors such as RANKL which can activate osteoclast precursors. Osteocytes activity are not limited to osteoclasts, and studies have shown that osteocytes can also affect osteoblasts [32]. Osteocytes are the main mechano-sensors in bone and are responsible for feedbacks to physical stimulation. For instance, they reduce the production of sclerostin which inhibits bone formation, in response to physical stimuli. Furthermore, the production of nitric oxide (NO), and cyclooxygenase 2 (COX2) in osteocytes are decreased due to mechanical stimulation [33]. COX2 have shown to promote osteoblasts formation, and NO considered to be a molecular messenger in bone intercellular activities [34].

In recent years, various studies have been conducted to investigate the relation between osteocytes activity and breast cancer cells. For example, Cui et al. have used the MLO-Y4 CM effect on MDA-MB-231 cells [31]. Based on their report, CM can prompt breast cancer cells proliferation. However, it will decrease their migration capacity. Furthermore, based on Ma et al. report MLO-Y4 CM reduce breast cancer cells apoptosis [35]. In a study conducted by Chen et al. the MLO-A5 cells which are another colon of osteocytes, were used to investigate the effect of CM on TMD spheroids [36]. Based on their report the MLO-A5 CM acts as an attractant for breast cancer cells. Furthermore, they showed that the CM could shrink cancer cells 3D spheroids, and suggest that osteocytes CM can reverse the EMT in cancer cells in the bone microenvironment by showing alternations in EMT associated protein expressions such as Snail downregulation. Several factors in osteocytes CM have been identified as the leading players in these behavior changes, including biglycan, osteonectin, and collagen. However, the underlying mechanism has remained unclear [36].

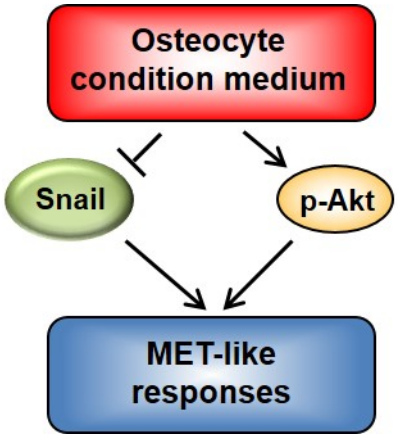

Fig. 1.2.: Osteocyte condition medium effect on TMD cells.

1.5 Fluid Flow as a Mechanical Stimulator

Bone metabolism is significantly affected by mechanical stimulation [37]. Studies have shown that by increasing mechanical stress, bone formation increases due to osteoblast activity. However, as it was mentioned before bone resorption and destruction is accelerated by different chronic or acute diseases such as cancer. Many studies have investigated the effect of mechanical load and strain on osteoblast-like cells. The results suggested that mechanical strain can stimulate osteogenesis [38]. The unmineralized matrix around the osteocytes in the bone form a porous structure which allows interstitial fluid to pass for nutrients and waste exchange. The pressure gradients due to compressive forces, stimulate the interstitial fluid through the lacunar-canalicular porosities which can generate shear stress between 0.8-3 Pa [39]. Therefore, one of the models that have attracted many interests for osteocyte mechanotransduction is fluid flow shear stress [40]. Studies have shown that osteoblasts and osteocytes can sense the fluid shear stress *in vitro*, and can generate osteocyte responses which are correlated with bone load *in vivo* [40]. For instance, production of prostaglandin E2 (PGE2) and NO, or inclined osteocytes apoptosis [41]. Two different mechanotransducers have been suggested in bone, which are ion channels and integrin adhesions [42]. Based on Burger et al. report shear stress can cause a rapid increase in intracellular calcium, which leads to the generation of PGE2 and NO, which both of them are associated with mechanical stimulation of bone formation *in vivo* [41]. By applying shear stress to osteocytes, focal adhesions related signals are also triggered, such as the interaction between αvβ3 integrin with Shc. In addition, PGE2 release in osteoblasts is blocked by soluble RGD peptides [43].

Based on Norvell et al. report β-catenin signaling is also affected and changed by fluid shear stress and mechanical stimulation [44].β-catenin plays an essential role in osteoblast differentiation and gene expression. The main reason behind this phenomenon has remained unclear, but some possible mechanisms have been suggested by different studies. For instance, N-cadherin has been shown to be downregulated

by fluid shear stress in osteocytes [44]. Cadherins that interact with β-catenin can regulate its signaling by inhibiting the β-catenin interaction between the plasma membrane and preventing its translocation. N-cadherin has shown to affect cell-differentiation signaling, including differentiation of cells to osteoblasts lineage [44].

As it was mentioned before, many growth factors are stored in bone. Growth factors are involved in many mechanisms in bone, including proliferation and differentiation of osteoblasts. Studies on human osteoblast-like cells and primary mouse osteoblastic cells have shown that fluid shear stress can alter some of these growth factors production. For instance, TGF-β production increases through cation channel function [37]. In addition, studies have shown that growth factors such as PDGFs, bFGF, and TGF-β mRNA expressions have increased in endothelial cells due to the fluid shear stress application [45, 46].

Studies have shown that by applying fluid shear stress to osteocytes *in vitro* and changes in bone microenvironment, also changes the cancer cells response. Based on Ma et al. report, the flow-stimulated osteocytes increase breast cancer cell apoptosis [35]. Furthermore, their migration assay results suggested that there is less affinity between flow-stimulated osteocytes CM and breast cancer cells compared to regular osteocytes CM. In addition, they showed that flow-stimulated osteocyte decline osteoclastogenesis. Even though the results suggested the anti-tumor potential of bone mechanical stimulation; the underlying mechanism is not well illustrated [35].

1.6 Mechanical Stimulation and Tibia Loading

Breast cancer mostly metastasis to cancellous bone, which is the load bearing section of the bone. Because of this, bed rest is prescribed for the patients who are diagnosed with a high risk of fraction [47]. However, bone microenvironment is very sensitive to mechanical stimulation, and lack of it leads to more bone loss. In contrast, by stimulating bone the osteoblast activity increases and result in increased bone production and mass [48]. Studies have shown that physical exercise can improve bone

strength, decrease bone loss rate, and can be used as adjuvant therapy in breast cancer patients. In addition, controlled mechanical loading has proven to have beneficial effects on bone *in vivo* model. For instance, tibia compression in different models such as OVX, hormone-deficient osteoporotic, and aged mice can stimulate bone formation in cancellous bone and prevent bone loss [49, 50]. It is important to note that, one of the essential parameters in the bone response to mechanical loading is the strain rate, and should be measured accordingly.

In a recent study conducted by Lynch et al. the effect of tibial compression on a bone metastases model was investigated [47]. Based on their report, SCID mice were injected with MDA-MB-231 human breast cancer cells to model the breast cancer bone metastases, and a 4.1 N compression load was used to make +600 strain at the medial midshaft of the tibia. 1200 cycles of loads were given at 4 Hz, 5 days/week. Their results showed, tibia compression significantly prevented tumor formation and prevented osteolytic bone loss in the loaded tibias. The effect of loading has been hypothesized that can be due to both changes in bone and cancer cells gene expressions and upregulation of osteoblastic over osteoclastic activity. However, the exact molecular mechanisms have remained unclear.

1.7 Question and Hypothesis

As it was mentioned before, studies have shown that breast cancer cells behave differently in the bone microenvironment. However, the effect of mechanical stimulation on bone microenvironment and its effects on tumor-bone interactions has not been well illustrated. In this study, we aimed to address this question: does apply mechanical stimulation to osteocytes changes migratory breast cancer cells behavior? To address this question both *in vitro* and *in vivo* models were used. In the *in vitro* model, MLO-A5 osteocytes were treated with the oscillatory fluid flow, and migration, proliferation, and gene expression alterations of TMD cells were studied in response to MLO-A5 conditioned medium with and without fluid flow treatment.

In the *in vivo* model, the breast cancer bone metastasis was modeled by tibia injection of 4T1.2 cells to BALB/c female mice. Furthermore, each mouse was treated with controlled tibia compression *in vivo*. Because of the Wnt signaling and Src involvement in cells mechanical responses, and their role in cellular proliferation and migration, we hypothesized that applying oscillatory fluid shear stress to osteocytes will lead to EMT-like responses in tumor cells. Moreover, we expected mechanical stimulation promote both migration and proliferation in breast cancer cells.

2. MATERIALS AND METHODS

2.1 *in vitro* Analysis

2.1.1 Osteocytes

The MLO-A5 osteocytes were cultured and grown in alpha-minimum essential medium (αMEM) (Gibco, Carlsbad, CA, USA) containing 5% fetal bovine serum (FBS), 5% fetal calf serum (FCS), and 1% antibiotics (50units/ml penicillin, and 50 μg/ml streptomycin; Life Technologies, Carlsbad, CA, USA). To keep the differentiation of the osteocytes, the cells were cultured in type I collagen treated (Cat No. 344236, BD Biosciences, San Jose, CA, USA) tissue culture dish (Corning). To apply fluid shear stress to the cells, it was needed to seed the cells on the glass slides. The glass slides were cleaned using MiliQ water and autoclaved to kill the remaining bacteria and remove potential contamination agents. Subsequently, the glass slides were coated with type I collagen solution (15 μg/ml, 0.02N acetic acid). After approximately one hour, the collagen was removed, and the glass slides were rinsed with 1x phosphate buffered saline (PBS) solution. The cells were incubated at 37°C temperature with 5% CO_2 incubator. To increase the effect of fluid flow on cells 3 hours before applying shear stress, the media was changed to 1% FBS αMEM. For the fluid flow, MLO-A5 CM containing 1% FBS was used.

2.1.2 Two-dimensional Scratch Assay

To perform the scratch assay, 12-well plates (Corning) were used. After preparation of the tumor cells, 4×10^5 cells were seeded per well, one day prior to the experiment using Dulbecco's modified eagle medium (DMEM) (Corning, Inc., Corning, NY, USA) containing 10% FBS and 1% antibiotics. The next day, before chang-

ing the medium to conditioned medium, each well was rinsed using plain DMEM. Subsequently, 1 mL of conditioned medium was added to each well. The scratch area was made with a plastic tip. The wound area was monitored, and images were taken at various time points. The wound area was measured with ImageJ. All of the two-dimensional scratch assays were done by Yao Fan.

2.1.3 Tumor Spheroids

Human breast cancer cell-derived cell lines, TMD cells were seeded in DMEM containing 10% FBS and 1% antibiotics. To seed tumor spheroids, after trypsinization and suspending cells in fresh medium, 200 μL of DMEM with a cell density of 25 cells/μL were added in a U-bottom low-adhesion 96 well plate (S-Bio, Hudson, NH, USA) and incubated in 37°C incubator with 5% CO_2. The medium was changed to conditioned medium after 24 hours. The tumor cells were monitored using an optical microscope and images were analyzed using ImageJ software. The images were taken on 12 and 24 hours' time points. All of the tumor spheroids assay were assisted by Yao Fan.

2.1.4 Three-dimensional Tumor-Bone Fusion Assay

Similar to tumor spheroid assay, MLO-A5 osteocytes, and TMD cells were trypsinized and prepared. Subsequently, cells were added to a U-bottom low-adhesion 96 well plate. MLO-A5 spheroids and TMD spheroids were formed in separated wells. After 48 hours, the culture medium was changed to conditioned mediums and spheroids were carefully transferred to other's well. The fusion was tracked using an optical microscope, and the cross-sectional area was measured with ImageJ. Three-dimensional tumor-bone fusion assay was done by Yao Fan.

2.1.5 Flow Chambers and Fluid Flow Characteristics

To apply oscillating fluid flow shear stress to the osteocytes, custom-made chambers with parallel plates with a custom-made machine were used. The machine includes a rotating motor around a fixed shaft, which created the forward and backward oscillating motion. The device stroke was controlled by changing the rotating axis offset from the fixed shaft. By connecting an air-sealed syringe to the moving axis of the device and connecting that to the tube containing MLO-A5 conditioned medium which was connected to the flow chamber, the oscillating fluid flow was produced. The flow chamber consists of a polycarbonate plate, a silicone rubber to seal the flow chamber, and a $75 \times 38\ mm^2$ glass slide which had the osteocytes monolayer on one side. The depth and area of the flow channel were approximately 300 μm and 28.5 cm^2, respectively. The fluid flow shear stress was calculated by approximate measurement of the flow rate in the tubes. To measure the shear stress that we applied to the MLO-A5 osteocytes, we assumed that the cell medium is a Newtonian fluid and the shear tensor is proportional to the deformation tensor. For steady flow between infinitely wide parallel plates, wall shear stress is calculated by:

$$\tau = \frac{6\mu Q}{bh^2} \tag{2.1}$$

In which, μ is the dynamic fluid viscosity, b is the width of the chamber and h is the height of it. Based on this equation, shear stress is a function of fluid flow rate (Q). For the experiment, the Tygon 3350 silicone tubes were used. The value of the medium viscosity at 37°C was obtained from the previous data [51]. Fluid flow was measured by approximate measurement of the fluid column change (δx) in the silicone tubes using a digital caliper (0.01 mm accuracy).

$$Q = A\delta x \tag{2.2}$$

In which A is the inner area of the silicon tube. Based on the companys catalog, the inner diameter of the silicon tubes was $\frac{1}{16}$ inch, and the δx was approximately 30 cm/s.

$$\mu = 0.72mPa, s = 0.72 \times 10^{-3} Pa.s \tag{2.3}$$

$$Diameter = D = \frac{1}{16}in = 0.16cm, radius = r = 0.08cm \tag{2.4}$$

$$A = \pi r^2 = 0.02cm^2 \tag{2.5}$$

$$Q = A\delta x = 0.59\frac{cm^3}{s} \tag{2.6}$$

$$b = 3.5cm, h = 0.03cm \tag{2.7}$$

$$\tau = \frac{6\mu Q}{bh^2} = \frac{6 \times 0.72 \times 10^{-3}[Pa.s] \times 0.59[\frac{cm^3}{s}]}{3.5 \times 0.03^2[cm^3]} = 0.81Pa \tag{2.8}$$

Prior to each experiment, the flow chambers were cleaned using 1% bleach, 70% ethanol, and MiliQ water and exposed to UV light for one hour. The silicone rubber which was used to isolate the flow chamber was autoclaved each time, to prevent the contamination. To investigate the flow and shear stress effect, 0.2 and 0.8 Pa were used. As a control for each experiment, one chamber was used with stabile medium inside the system. After one hour of flow, the MLO-A5 conditioned mediums and proteins were extracted.

2.1.6 Plasmid and si-RNA Transfection

To overexpress the Snail expression in TMD cells, a plasmid consisting of Snail coding sequence (SnailHA-pcDNA3; Addgene, Cambridge, MA, USA) was used. The control group was treated with an empty plasmid vector (FLAG-HA-pcDNA3.1; Addgen). Moreover, to inhibit Src expression, TMD cells were treated with si-RNA specific to Src. A negative si-RNA (Silencer Select #1, Life Technologies) was used for the control group. To transiently transfect the cells, si-RNA was used in Opti-MEM I medium with Lipofectamine RNAiMAX (Life Technologies). After 24 hours, the efficiency of si-RNA transfection and plasmid vectors were evaluated by western blot. Plasmid and si-RNA transfection were assisted by Yao Fan.

2.2 *in vivo* Analysis

2.2.1 Animal Preparation

For this study, 17 BALB/c (6 weeks old) female mice were used. The animals were housed four to five per cage and provided with mouse chow and water ad libitum at the Indiana University Animal Care Facility in light/dark controlled room. All the experimental procedures were approved by Indiana University Animal Care and Use Committee and were in compliant with the Guiding Principles in the Care and Use of Animals endorsed by the American Physiological Society. Animals were weighed each day prior to the treatment until sacrifice to evaluate the general health. A summary of the experimental procedure and timeline is provided in Figure 2.1.

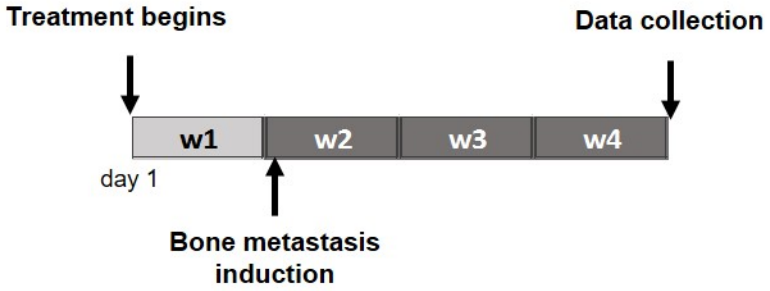

Fig. 2.1.: Timeline of the experimental protocol.

2.2.2 Preparation of Tumor Cells

4T1.2 mouse mammary tumor cells (Dr. R. Anderson, Peter MacCallum Cancer Institute, Melbourne, Australia) were cultured in DMEM containing 10% FBS and 1% penicillin antibiotics (Life Technologies, Grand Island, NY, USA). The cells were treated with type I collagen (Corning, NY, USA) and incubated at 37°C and 5% CO_2 humidified incubator. Before the surgery, cells were trypsinized and, suspended in 1x PBS solution (10^4 cells/μl) .The cells were kept in ice at 4°C before injection.

2.2.3 Bone Metastasis Induction

For the bone metastasis induction, animals were anesthetized using 3% isoflurane, and the gas flow rate was 0.5-1.0 ml/min. Before the injection, the operation site was cleaned using 70% ethanol and 10% povidone-iodine. To induce bone metastasis in the tibia bone, knee has been placed in the flexed position, and 20 μL of 1x PBS solution with a cell density of 2.5×10^4 4T1.2 cells/μL was injected directly to the left tibia plateau using 1 mL insulin syringe while the needle was placed in the marrow space of the proximal compartment. Animals were given 3 days to recover after the surgery. All the injections were done by Yao Fan.

2.2.4 Tibia Loading

The tibia loading was performed using Electro Force 3100 (Bose, Inc, Framingham, MA, USA). Animals were anesthetized prior to the treatment using an anesthetic induction chamber using 2.5% isoflurane, with approximately 1 ml/min flow rate. Animals were mask anesthetized during the procedure. The loads were applied in the axial direction. The left foot was placed on a custom made piezoelectric, and both foot and the knee joint were fixed. The loads were given every day, 5 minutes every other day for three weeks using 2 N force (peak-to-peak) at 2 Hz. These conditions were chosen based on the previous studies [47]. For the placebo group, animals were anesthetized for 5 minutes in the anesthetic induction chamber and carefully returned to the cage.

2.3 Data Analysis Procedure

2.3.1 X-ray Imaging

The X-ray images were taken in the Indiana University Animal Care Facility using Device Faxitron. The imaging process begun after the device calibration. The harvested bones were thawed at the room temperature. Each bone was placed on the

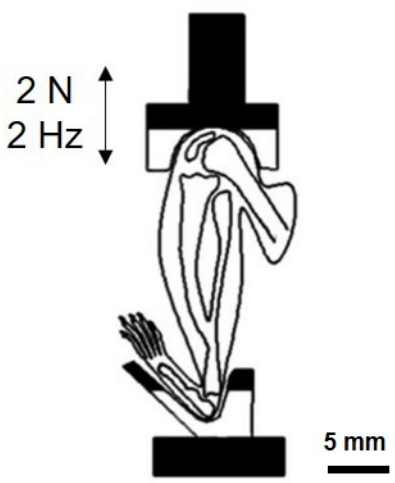

Fig. 2.2.: Diagram of tibia between loader and stator, from the side [52].

device platform carefully, and images were taken and recorded. After determination of region of interest, the images contrast was adjusted using the manufacturer provided software.

2.3.2 Area and Roughness of Tumor Spheroids

To evaluate the morphological changes in TMD spheroids, images were taken with the optical microscope at 18 and 24-hour time points after cultivation. The spheroid images were imported to the ImageJ (v1.51) software and analyzed. Based on the microscope resolution, each pixel equaled 950 mm. Using Java code, the tumor spheroid area was measured based on the light contrast. The tumor spheroid roughness was calculated based on the tumor ellipse and intersect using the formula below:

$$Roughness = \frac{tumor\ spheroid\ area + tumor\ ellipse - 2 \times tumor\ intersect}{tumor\ spheroid\ area} \quad (2.9)$$

2.3.3 EdU and MTT Analysis

Tumor cells proliferation rate is one of the important factors that indicates tumor progression. To investigate the proliferation in response to different conditioned mediums, a fluorescence-based cell proliferation kit was used (Click-iT EdU Alexa Fluor 488 Imaging Kit; Thermo-Fisher). The cells were seeded 24 hours prior to EdU incubation. 3 hours after incubating with EdU, the cells were fixed according to manufacturer provided protocol. Later on, using a confocal microscope (Olympus, Tokyo, Japan) images were taken, and analyzed by ImageJ.

The MTT analysis was performed to study how the conditioned medium can affect the tumor cells number and population. A 96 well plate (Corning) and MTT cell proliferation kit (Invitrogen, Carlsbad, CA, USA) were used. 20μL of TMD cells suspension in 10% FBS DMEM with a cell density of 150 cells/μL was added to each well. For each group, 5 wells were used for statistical analysis. After the first day of seeding, the medium was changed. 2 days after changing the medium, the MTT solutions were added, and the optical density of the solutions was read by EL800 (BioTek). Subsequently, the data were normalized and analyzed. Both MTT and EdU analysis were partially assisted by Yao Fan.

2.3.4 Western Blot Analysis

To see how the conditioned mediums change the cells protein expressions, TMD cells were seeded in a 6-well plates (Corning), 2×10^5 cells/well, one day prior to medium exchange. The cells were cultured in DMEM containing 10% FBS, and 1% antibiotics. Before exchanging the mediums to conditioned mediums, each well was rinsed with plain DMEM.

To extract the proteins from the cells radioimmunoprecipitation assay (RIPA) buffer solution containing phatase (Santa Cruz Biotechnology, Santa Cruz, CA, USA) and protease inhibitors (Cadlibiochem, Billerica, MA, USA) was used to lyse the cells. In addition, the protein solution was sonicated to lyse the remaining cells in the solu-

tion. Subsequently, the extracted proteins were separated using 10% SDS gels during gel electrophoresis procedure and transferred to Immobilon-P membranes (Millipore, Billerica, MA, USA). The membranes were cut based on the protein weight and incubated with the first antibody. The first antibody incubation time was dependent on the protein type. Afterwards, the membranes were incubated with either anti-rabbit or anti-mouse IgG conjugated with horseradish peroxidase for 45 minutes. Proteins were detected using SuperSignal West Femto maximum sensitivity substrate (Thermo Scientific). The images were analyzed by a luminescent image analyzer (LAS-3000, Fuji Film, Tokyo, Japan). All of the western blot figures were supported by Yao Fan.

2.3.5 ELISA Analysis

It was hypothesized that TGF-β could be one on the potential stimulators of the changes in TMD cells behavior. To measure the concentration of TGF-β in the conditioned mediums a TGF-β ELISA kit (TGF beta-1 Human/Mouse Uncoated ELISA Kit, Thermo Scientific) was used. A 96 well plate (Corning) was used for 4 groups of samples; standard solution, control, MLO-A5 CM, and MLO-A5 FFCM. The procedure was done based on the manufacturer provided instruction. 30 minutes after adding ELISA solution, the optical density of the solutions was read by EL800 (BioTek). Subsequently, after normalization of the optical densities based on the manufacturer provided standard solution, the TGF-β concentration in samples was calculated.

2.3.6 Fluorescence Resonance Energy Transfer (FRET)

To monitor the Src activities in lipid rafts of plasma (Lyn-Src), and the cytosol (Cyto-Src), FRET-based, cyan fluorescent protein (CFP)-yellow fluorescent protein (YFP) biosensors were used. A Cyto-Src includes four main components which are CFP, YFP, a truncated Src substrate peptide, and an effector protein binding domain. Lyn-Src is synthesized by the combination of Lyn kinase and N-terminal of Cyto-Src

biosensor. Src activation leads to increased interaction and binding of the effector protein binding domain to the truncated Src domain. These interactions cause a conformational change in the biosensor and incline the FRET efficiency from CFP to YFP. Therefore, Src activity can be monitored by changes in the emission ratio of the CFP to YFP.

A Nikon Ti-E inverted microscope was used for taking images. Three filters were used for the imaging process including YFP (FRET) emission (542/27), CFP excitation (438/24), and CFP emission (483/32). To maintain the focus during time-lapse imaging, the microscope was equipped with a Perfect Focus System (Nikon). In addition, a 100 W Hg lamp with an ND64 neutral density filter was used to lessen photobleaching. To generate Src activity FRET images, the emission ratio of CFP/YFP for a single cell was measured by NIS-Elements software (Nikon). To quantify the Src activity based on the FRET responses, the discrete time associated derivatives of the emission ratios, Y, was calculated. It was assumed that the rate of FRET ratio change in response to cytokines follows a Gaussian distribution. Furthermore, Y related curve was fitted using Gaussian functions:

$$Y = A \times \exp(\frac{-0.5 \times (t - \mu)}{\sigma^2}) \tag{2.10}$$

In which A is the maximal rate of FRET ratio, μ is the time when the rate of FRET ratio change reaches the maximal value, and σ is the duration of the rate of FRET ratio change.

2.3.7 Mechanical Testing (*in vivo* and *ex vivo*)

After euthanasia tibia was harvested and kept in 1x PBS solution at -20°C freezer. Before mechanical testing, tibia bones were brought to the room temperature and kept in 1x PBS solution to keep hydrated. To evaluate tibia bone mechanical properties, *in vivo*, and *ex vivo* assessments were performed. For all the mechanical evaluations Electro Force 3100 device was used. 2 days in each week were chosen to evaluate

the tibia stiffness *in vivo* by axial loading measurement. The test was performed on Tuesdays and Fridays of each week until sacrifice. After sacrifice, both axial stiffness and bending stiffness were measured. To evaluate the bending stiffness, standard 3-point bending method was used. Briefly, bones were thawed at the room temperature. Subsequently, the tibia length was measured from the intercondylar eminence to medial malleolus using a 0.01mm caliper. The posterior midshaft was marked, and bone was fixed from proximal and distal tibia points. An oscillating 1N peak-to-peak force, with 1Hz frequency, was applied for 15 seconds to the medial midshaft of the tibia in the anterior-posterior direction. The support span length was 6 mm. To measure the axial stiffness, two rounded-top mounts were used on the machine. The intercondylar eminence and medial malleolus of the tibia were fixed on the mounts, and the loads were given in the axial direction with the previously described characteristics.

The displacements and the force changes were recorded using the manufacturer software. To calculate the stiffness, the force-displacement data was imported to MATLAB. The bone stiffness was calculated based on the force-displacement curve in a specific force range where the curve changes were linear. The mechanical loads were applied five times in each run, and the average stiffness from the last three times was measured and presented as the bone's stiffness. All the process were performed using a custom-made MATLAB script.

2.3.8 Micro-CT

Miro computed topography images were taken using Skyscan 1170, at Indiana University School of Medicine. All the bones were brought to the room temperature and wrapped in Parafilm to keep hydrated. The images were taken with a medium sized camera with 8.9 voxel resolution. Two hydroxyapatite phantoms (0.25 and 0.75 g/cm^3) were used for calibration, to measure the bone mineral density (BMD) and grayscale values. The images were reconstructed and rotated using NRecon v1.6.9.15

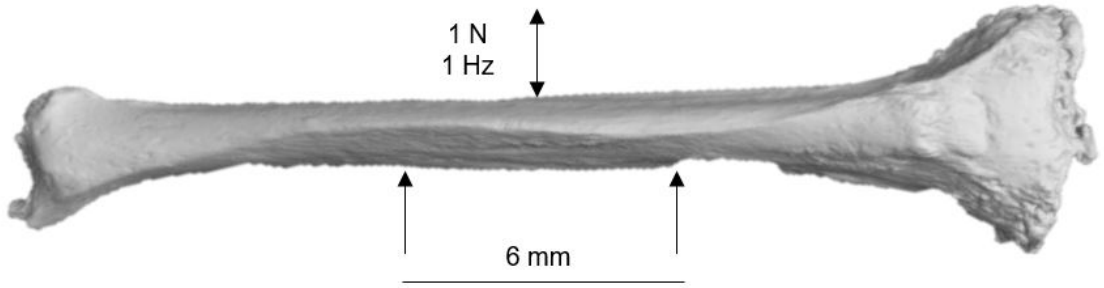

Fig. 2.3.: Diagram of tibia mechanical testing and span size.

and DataViewer v1.5.0 software, respectively. The regions of interest were manually determined for trabecular and cortical bones, and the analysis was performed using CTAn v1.11.4.2 software. Cancellous volume of interest was determined 0.5mm distal to the growth plate and extended to 10% of the tibia length [53].

2.4 Statistical Analysis

For all the quantitative data, the standard deviation and mean were calculated. For statistical group comparisons, the Students t-test was used. The post hoc values were used as the primary tool to detect significant differences between groups. The statistical significances have been shown using (*) and (**) for p-values less than 0.05 and 0.01, respectively. The outliers were detected and removed by Grubbs' test when the significance probability was less than 0.05.

3. RESULTS

3.1 Effect of MLO-A5 CM on TMD Cells

3.1.1 MLO-A5 CM Inhibited TMD Cells Migration

To investigate how MLO-A5 CM alters the TMD cells migration behavior, 2-dimensional wound healing scratch assay was conducted. As the Figure 3.1 shows, the results revealed that the MLO-A5 CM inhibited the TMD cells migration. The results showed that the wound area of the samples, which were treated with MLO-A5 CM, was significantly larger than the control samples. At 24-hour time point, the average wound area of the treated samples was 92% larger than the control group ($p<0.05$).

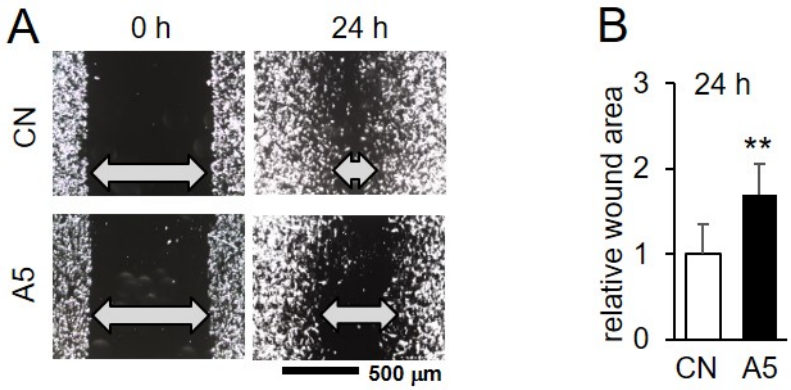

Fig. 3.1.: Effect of MLO-A5 CM on TMD cell migration. (A&B) Lower motility of TMD cells in the presence of MLO-A5 CM.

3.1.2 MLO-A5 CM Decreased Tumor Spheroid Area and Roughness

As the second indicator of behavior and morphology changes of TMD cells in the presence MLO-A5 CM, 3-dimentional tumor spheroid assay was conducted. As the Figure 3.2 shows, after 24 hours, the mean tumor spheroid area of the MLO-A5 CM treated group was significantly smaller than the control group. The mean tumor spheroids roughness was also measured. Even though no statistically significant changes were seen in the spheroids roughness, the trend was consistent with the spheroids area.

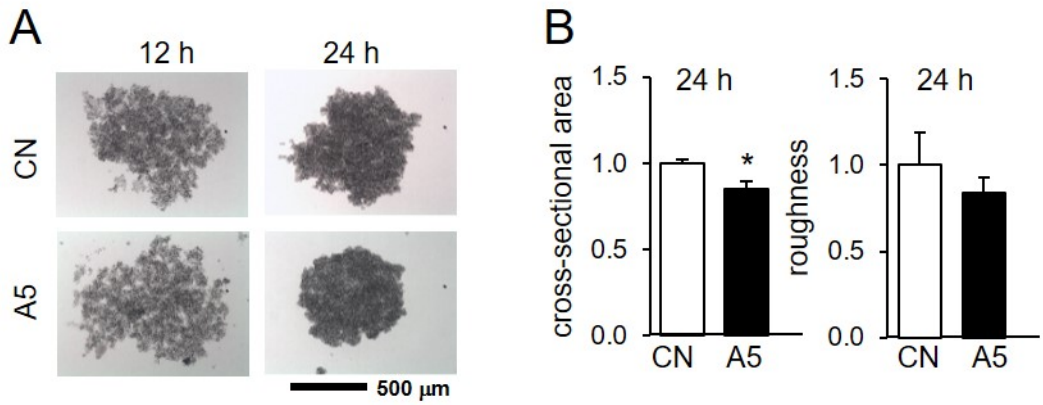

Fig. 3.2.: Effect of MLO-A5 CM on TMD spheroids formation. (A) Representative images of TMD spheroids with and without the presence of MLO-A5 CM. (B) Two spheroid parameters (cross-sectional area, and roughness).

3.1.3 Protein Expression, and Cell Proliferation Analysis

To investigate how MLO-A5 CM is affecting the TMD cells protein expressions related to EMT, expression of proteins including Snail, p-Akt, and Akt were measured through western blotting. The results revealed that the Snail expression of TMD cells is downregulated after incubation with MLO-A5 CM. On the contrary, Akt and p-Akt

were both upregulated by the MLO-A5 CM. The β-actin expression was consistent through all the samples.

By using EdU assay relative cell growth and proliferation of TMD cells in the presence of MLO-A5 CM was compared to no treated group. The results illustrated that MLO-A5 CM increased TMD cells proliferation. As it is shown in Figure 3.3, the relative proliferation of TMD cells was increased close to 10% in the presence of MLO-A5 CM ($p<0.05$).

Moreover, MTT assay was conducted to study the effect of MLO-A5 CM on TMD cells growth and proliferation. As the results in Figure3.3 show, the TMD cells proliferation is significantly increased in MLO-A5 CM. Based on the results, the proliferation of tumor cells in osteocytes conditioned medium increased up to more than 70% ($p<0.01$).

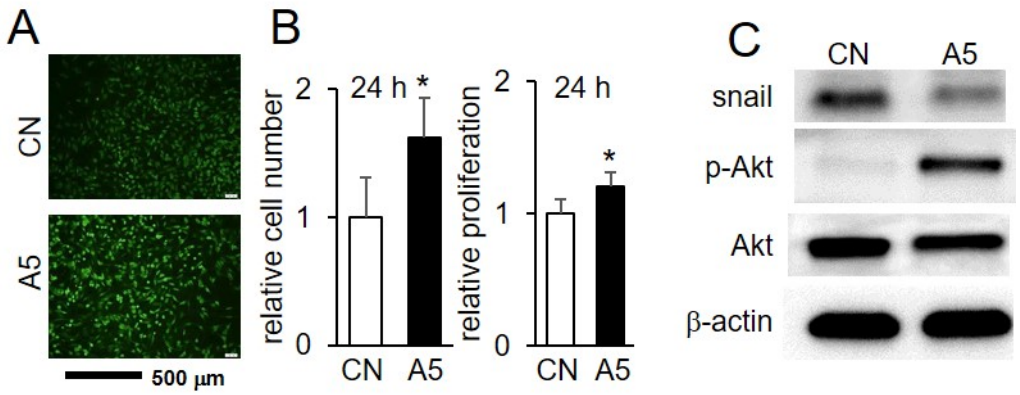

Fig. 3.3.: Effect of MLO-A5 CM on TMD cells protein expression, cell growth, and proliferation. (A) Representative images of fluorescence EdU cell proliferation assay in the presence of MLO-A5 CM. (B) MLO-A5 CM increased both TMD cells relative growth, and proliferation. (C) Protein levels of Snail, p-Akt, and Akt in response to MLO-A5 CM.

3.2 Effect of MLO-A5 FFCM on TMD Cells

3.2.1 MLO-A5 FFCM Promoted TMD Cells Migration

To investigate the migratory behavior of TMD cells with MLO-A5 FFCM and compared it to MLO-A5 CM, the 2-dimensional motility scratch assay on TMD cells using both MLO-A5 conditioned medium with and without fluid flow treatment was conducted. The results revealed that opposite to MLO-A5 CM, MLO-A5 FFCM promoted tumor cells migration. Based on the results which are shown in Figure 3.4 the wound area of TMD cells which were treated with MLO-A5 FFCM (0.8 Pa) was 34% smaller than the no-flow group (0 Pa) after 24 hours ($p<0.05$).

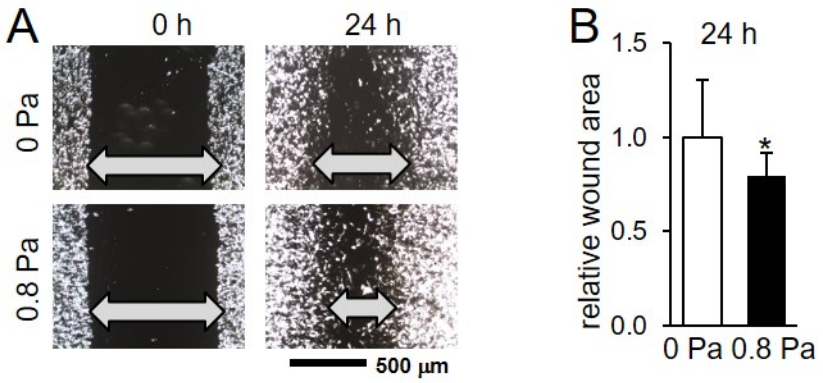

Fig. 3.4.: Effect of MLO-A5 FFCM on TMD cells migration. (A&B) Higher motility of TMD cells in the presence of MLO-A5 FFCM compare to no-flow treated conditioned medium.

3.2.2 MLO-A5 FFCM Increased Tumor Spheroid Area and Roughness

3-dimensional tumor spheroid assay was used as another indicator of tumor cells migratory behavior in response to the conditioned medium. The morphology changes of 3D tumor spheroids were screened for 24 hours. The area of tumor spheroids which

were treated with MLO-A5 FFCM (0.8 Pa) was significantly larger than the no-flow treated group ($p<0.05$).

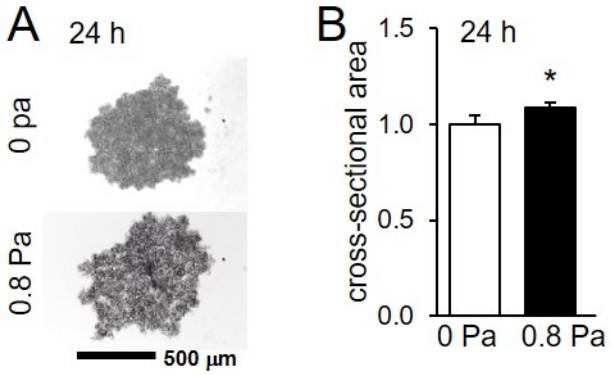

Fig. 3.5.: Effect of MLO-A5 FFCM on TMD spheroids formation. (A) Representative images of TMD spheroids in the presence of MLO-A5 CM with and without fluid flow treatment. (B) Higher cross-sectional area of TMD spheroids in the presence of MLO-A5 FFCM compare to no-flow treated samples.

3.2.3 Protein Expression, and Cell Proliferation Analysis

As it is shown in Figure 3.6. the western blot protein analysis results revealed that compared to no flow, Snail expression of TMD cells is upregulated by MLO-A5 FFCM. The p-Akt and Akt expressions were also measured, and results showed that when MLO-A5 osteocytes are treated with oscillating fluid flow shear stress the conditioned medium can downregulate the p-Akt expression of tumor cells in opposite to MLO-A5 CM. The Akt expression has remained constant, and β-actin had the same expression level, and it was consistent for both groups.

Consistent to p-Akt downregulation, the MTT and EdU assays results revealed that TMD cells proliferation, and growth were also decreased significantly in the presence of MLO-A5 FFCM. As the Figure 3.6 shows, the cell number of tumor

cells in the presence of MLO-A5 FFCM was 40% smaller than no-flow treated group ($p<0.01$).

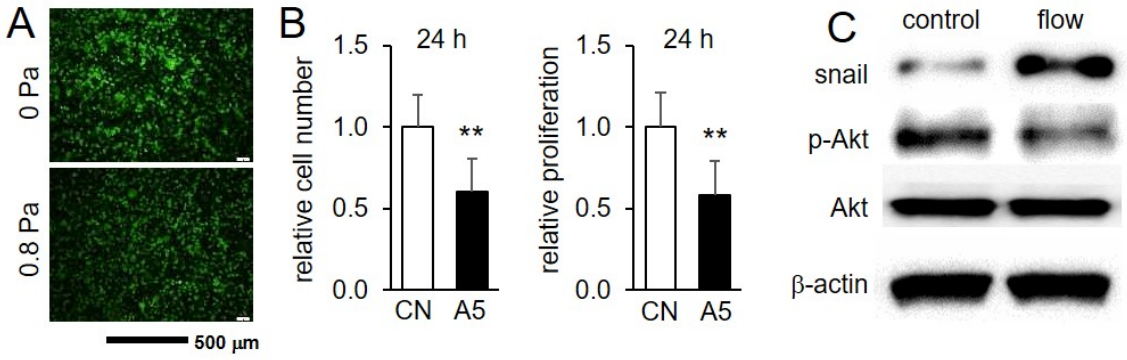

Fig. 3.6.: Effect of MLO-A5 FFCM on TMD cells protein expression, cell growth, and proliferation. (A) Representative images of fluorescence EdU cell proliferation assay in the presence of MLO-A5 FFCM. (B) MLO-A5 FFCM decreased both TMD cells proliferation, and relative population. (C) Protein levels of Snail, p-Akt, and Akt in response to MLO-A5 FFCM.

3.3 Effect of MLO-A5 FFCM with Lower Fluid Flow Shear Stress

To study the effect of fluid flow shear stress on MLO-A5 osteocytes and its interactions with TMD cells more deeply, the experiment was conducted with the same procedure. However, the fluid flow shear stress was decreased to 0.2 Pa.

3.3.1 MLO-A5 FFCM Promoted TMD Cells Migration

A 2-dimensional scratch motility assay was conducted on TMD cells using the flow and no-flow treated conditioned mediums. The results revealed that after 24 hours TMD cells which were treated with FFCM had significantly smaller wound area. As

the results are shown in Figure 3.7. The wound area of MLO-A5 FFCM (0.2 Pa) was 33% smaller than no-flow treated (0 Pa).

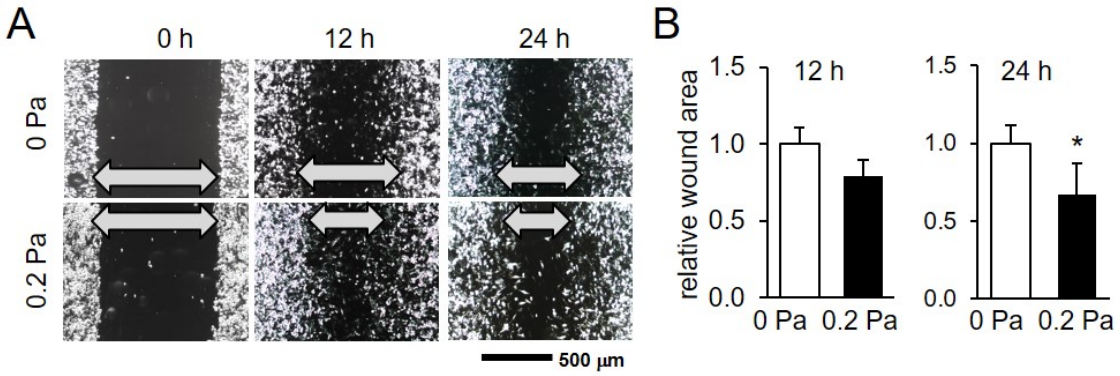

Fig. 3.7.: Effect of low shear stress MLO-A5 FFCM on TMD cells migration. (A&B) Higher TMD cells motility in the presence of low shear stress MLO-A5 FFCM compare to no-flow treated MLO-A5 CM based on a 2-dimensional scratch assay.

3.3.2 Protein Expression, and Cell Proliferation Analysis

To further examine the effect of low shear stress MLO-A5 FFCM on TMD cells, MTT and protein analysis were also performed. The results revealed that the effect of MLO-A5 FFCM on tumor cells proliferation, with both high and low shear stresses (0.2 and 0.8 Pa) is the same. As the Figure 3.8 shows, the MLO-A5 FFCM with 0.2 Pa shear stress has also decreased the growth and proliferation of tumor cells. Moreover, the western blot analysis showed that Snail expression is upregulated due to the use of MLO-A5 FFCM, and p-Akt expression is downregulated.

3.4 Effect of MLO-A5 Conditioned Mediums on 4T1 Cells

The effect of MLO-A5 FFCM on TMD cells, showed interesting results. However, different cancer cell types might react differently to the conditioned medium. To

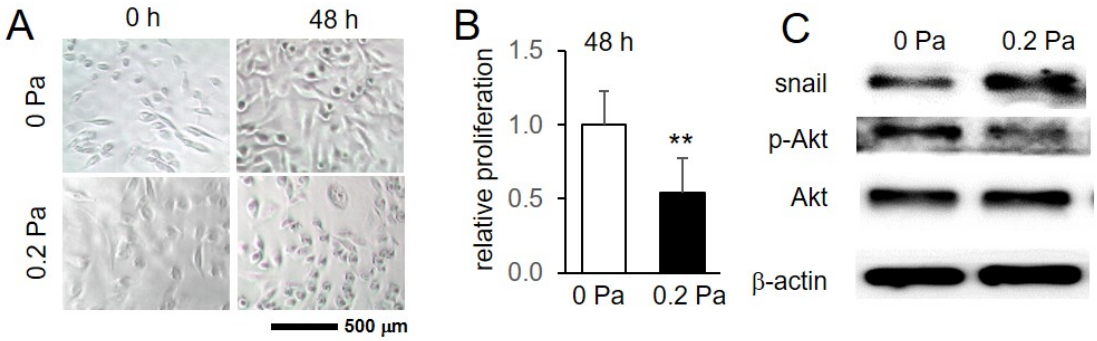

Fig. 3.8.: Effect of low shear stress MLO-A5 FFCM on TMD cells protein expression, and cell proliferation. (A) Representative images of TMD cells proliferation in the presence of low shear stress MLO-A5 FFCM, at 0 and 48 hours time points based on MTT assay. (B) Lower relative TMD cells proliferation in the presence of lower shear stress MLO-A5 FFCM. (C) Protein levels of Snail, p-Akt, and Akt in response to low shear stress MLO-A5 FFCM.

investigate the effect of MLO-A5 conditioned mediums on other cell types, the same assays were replicated using 4T1 cells.

3.4.1 MLO-A5 CM Inhibited 4T1 Cells Migration

As it was mentioned before, MLO-A5 conditioned medium inhibited TMD cells migration. The same 2-dimensional scratch motility assay was conducted on 4T1 cells. The results showed that after 12 hours the control group of 4T1 cells had significantly smaller wound area than MLO-A5 conditioned medium treated group. As it is shown in Figure 3.9. 4T1 cells behave comparable to TMD cells in this assay.

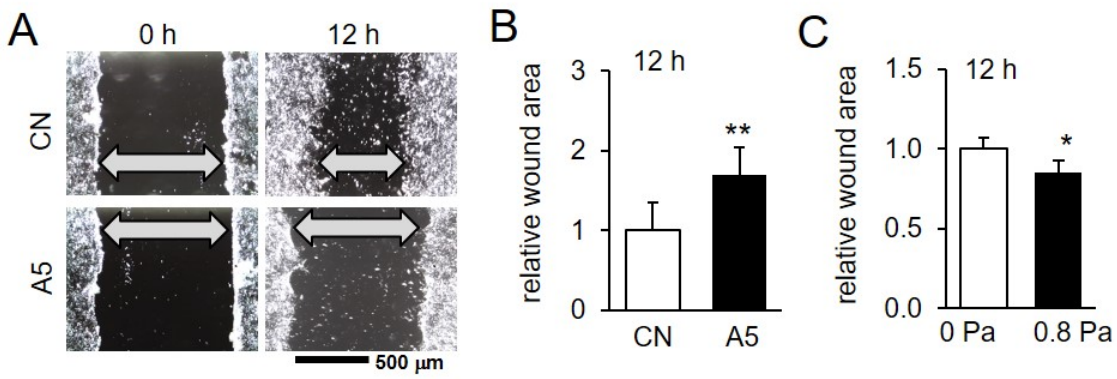

Fig. 3.9.: Effect of MLO-A5 CM and FFCM on 4T1 cells migration. (A&B) Lower motility of 4T1 cells in the presence of MLO-A5 CM based on 2-dimensional scratch assay. (C) Smaller wound area of 4T1 cells in the presence of MLO-A5 FFCM compared to no-flow treated conditioned medium based on 2-dimensional scratch assay.

3.4.2 MLO-A5 FFCM Promoted Migration in 4T1 Cells

2-dimensional wound healing scratch assay was conducted on 4T1 cells using MLO-A5 FFCM and no-flow treated MLO-A5 CM. The results indicated that 4T1 cells behave similar to TMD cells, and MLO-A5 FFCM increased the 4T1 cells motility compare to no-flow treated conditioned medium. After 12 hours, the relative wound area of the no-flow treated conditioned medium was 15% larger than the MLO-A5 FFCM.

3.4.3 Protein Expression, and Cell Proliferation Analysis

As it is shown in Figure 3.10, MTT analysis results revealed that MLO-A5 FFCM also decreased the proliferation rate in 4T1 cells. In addition, Snail, p-Akt, and Akt protein expressions in 4T1 cells were measured in response to flow and no-flow treat MLO-A5 conditioned medium. As similar to TMD cells, the results showed that

the Snail protein expression was downregulated by MLO-A5 CM, and upregulated by MLO-A5 FFCM. On the contrary, p-Akt expression was downregulated by no-flow treated MLO-A5 CM and upregulated by MLO-A5 FFCM. Akt expression was similar in both groups and no differences were seen.

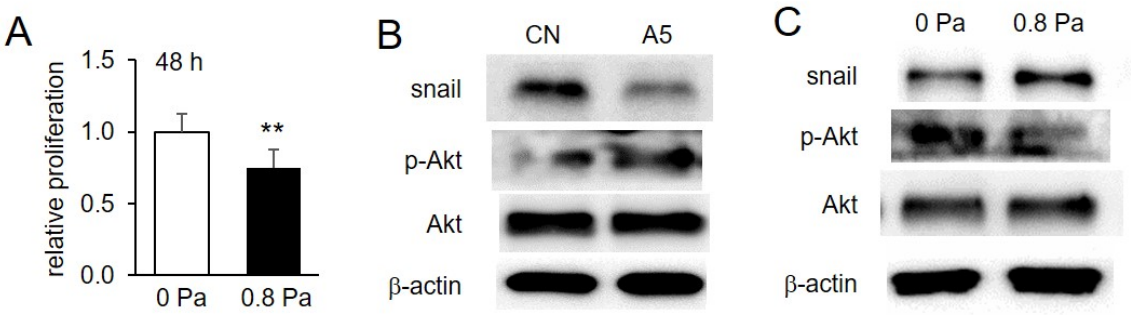

Fig. 3.10.: Effect of MLO-A5 conditioned mediums on 4T1 cells protein expression, and proliferation. (A) Decreased proliferation of 4T1 cells in the presence of MLO-A5 FFCM based on MTT assay. (B) Protein level of Snail, p-Akt, and Akt of 4T1 cells in response to MLO-A5 CM, and FFCM.

3.5 Wnt Signaling

As it was mentioned before, one of the possible reasons for EMT in breast cancer cells is the activation of Wnt signaling. To investigate this phenomena, Wnt3a which is a canonical Wnt signaling pathway activator, and XAV-939 which is a Wnt signaling inhibitor were used.

3.5.1 Effect of Wnt Signaling on Tumor Spheroid Area and Roughness

To study the effect of Wnt signaling on 3-dimensional tumor spheroids and comparison to MLO-A5 CM, and FFCM, Wnt activator and inhibitor were added to TMD cells culture medium. The result revealed that the addition of Wnt3a increased tumor

spheroid area and roughness significantly. Furthermore, XAV significantly decreased tumor spheroid area, however, there was no significant difference in their roughness. These results suggested that in the presence of Wnt3a, tumor cells behaved more migratory. In addition, by inhibiting Wnt signaling in TMD cells, they became more stationary.

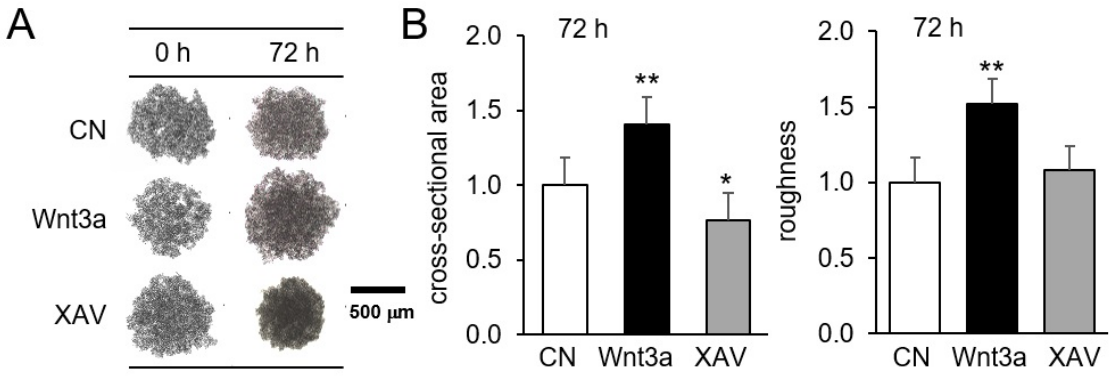

Fig. 3.11.: Effect of Wnt signaling on TMD spheroids formation. (A&B) Representative images of TMD spheroids, Wnt3a and XAV treated TMD cells after 72 hours. (B) Changes in two spheroid parameters (cross-sectional area, and roughness, respectively) by Wnt3a and XAV after 72 hours.

3.5.2 Effect of Wnt Signaling on TMD Cells Migration

2-dimensional wound healing scratch assay was performed by along with the addition of Wnt3a and XAV to the TMD cells culture medium, in order to further analysis the effect of Wnt signaling on tumor cells behavior. As it is shown in Figure 3.12 after 24 hours the relative wound area of the Wnt3a treated group was significantly smaller than the control group, and as the previous 3-dimensional tumor spheroid data indicated, Wnt3a promoted migration in TMD cells. Furthermore, the relative wound

area of XAV treated group was 20% larger than the control group, and inhibition of Wnt signaling decreased tumor cells motility.

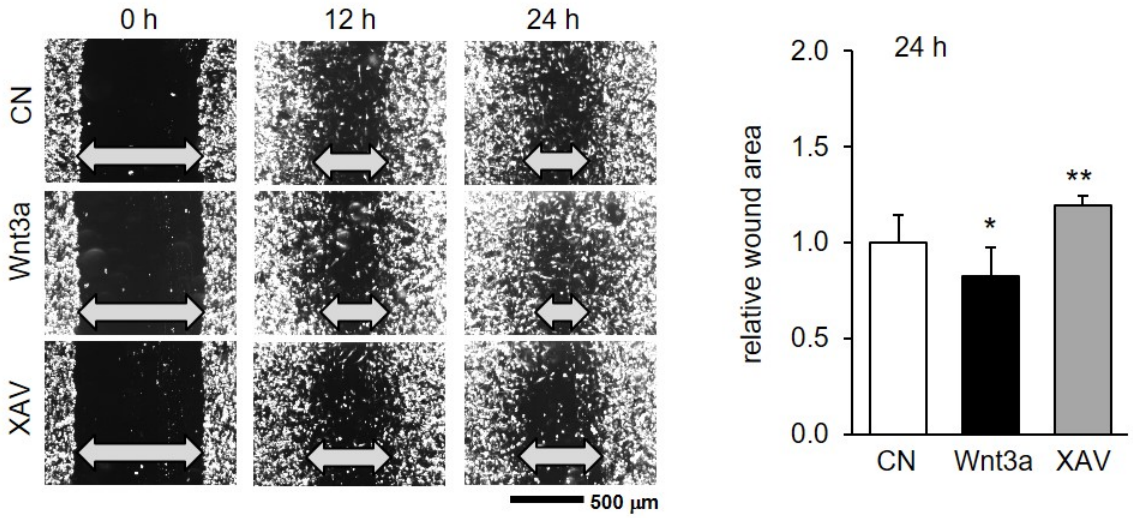

Fig. 3.12.: Effect of Wnt signaling on TMD cells motility and migration. (A&B) Promotion and inhibition of TMD cells migration by Wnt3a and XAV, respectively.

3.5.3 Protein Expression, and Cell Proliferation Analysis

The results from MTT analysis showed that Wnt signaling can also alter the proliferation rate in tumor cells. As the results in Figure 3.12 show, by blocking Wnt signaling the relative proliferation of TMD cells was decreased more than 30% ($p<0.01$). On the other hand, results indicated that by stimulating and activating Wnt signaling by Wnt3a, relative proliferation of tumor cells increased significantly ($p<0.05$).

To compare the effect of Wnt signaling with MLO-A5 CM, and FFCM, TMD cells Wnt signaling associated protein expression levels were measured through western blotting. Based on the results, Snail, and p-Akt expressions were upregulated by Wnt3a and down-regulated by XAV. On the contrary, Lrp5 expression was down-

regulated by Wnt3a and upregulated by XAV. The Akt expression was similar in all groups. In addition, the TMD cells Lrp5 expression was downregulated by MLO-A5 conditioned medium. Furthermore, the results revealed that Lrp5 expression level was upregulated by MLO-A5 FFCM. However, β-catenin expression level which is one of the main proteins in Wnt signaling pathway is slightly downregulated by MLO-A5 FFCM. No significant change was seen in p-β-catenin and p-NFκB expression levels.

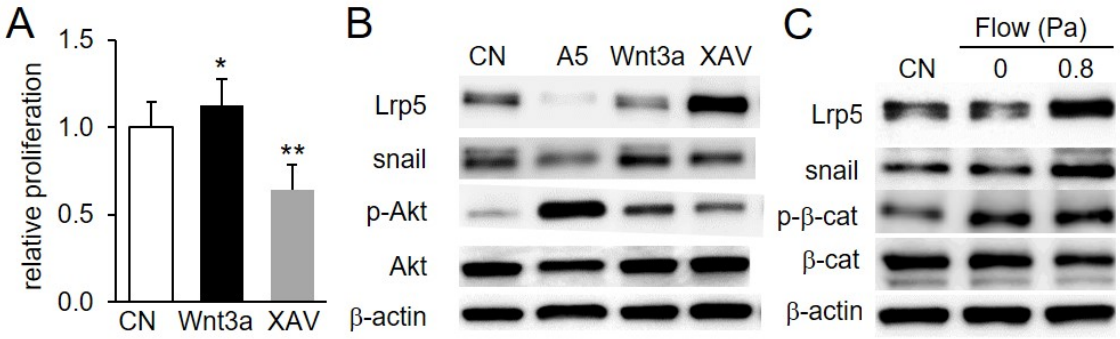

Fig. 3.13.: Effect of Wnt signaling on TMD cells protein expression, and proliferation. (A) Increased relative proliferation of TMD cells by Wnt3a, and decreased by XAV based on MTT assay. (B) Protein level of Wnt signaling associated proteins of TMD cells in response to Wnt3a and XAV. (C) Protein level of Wnt signaling associated proteins of TMD cells in response to MLO-A5 CM, and FFCM.

3.6 Src and Snail Pathways

3.6.1 Effect of MLO-A5 CM on Src Expression

Snail expression in tumor cells has shown to be upregulated by MLO-A5 FFCM. As it was mentioned before Snail is one of the main proteins indicating EMT in cancer cells. To further understand the mechanism behind the EMT in TMD cells due to

incubation with MLO-A5 FFCM, the Src, and FAK expressions of TMD cells were measured in response to MLO-A5 CM, and FFCM. Based on the results p-Src was downregulated in tumor cells by MLO-A5 conditioned medium. However, no changes were seen in the FAK or p-FAK expressions. Moreover, the results indicated that p-Src is upregulated by the MLO-A5 FFCM, but FAK and p-FAK expressions were not changed by the flow treated conditioned medium.

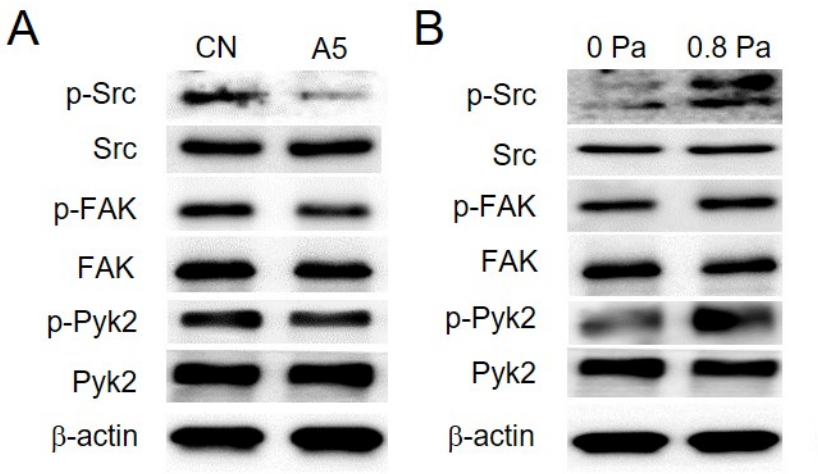

Fig. 3.14.: Effect of MLO-A5 CM, and FFCM on Src and FAK expressions. (A&B) Protein level of Src and FAK of TMD cells in response to MLO-A5 CM, and FFCM.

3.6.2 Src and Snail Pathway

Since the changes in expression of Snail and Src in TMD cells in response to conditioned mediums were similar, the relation between Src and Snail was investigated. For this purpose, Snail plasmid and si-RNA specific to Src were used. The results revealed that Src is upstream of Snail. As it can be seen in Figure 3.15, by Snail plasmid transfection, Snail expression is upregulated, however, no changes in p-Src and Src were detectable. In contrary, the results showed that by Src knockdown,

Snail expression is inhibited. Furthermore, Src knockdown promoted Lrp5 expression in TMD cells.

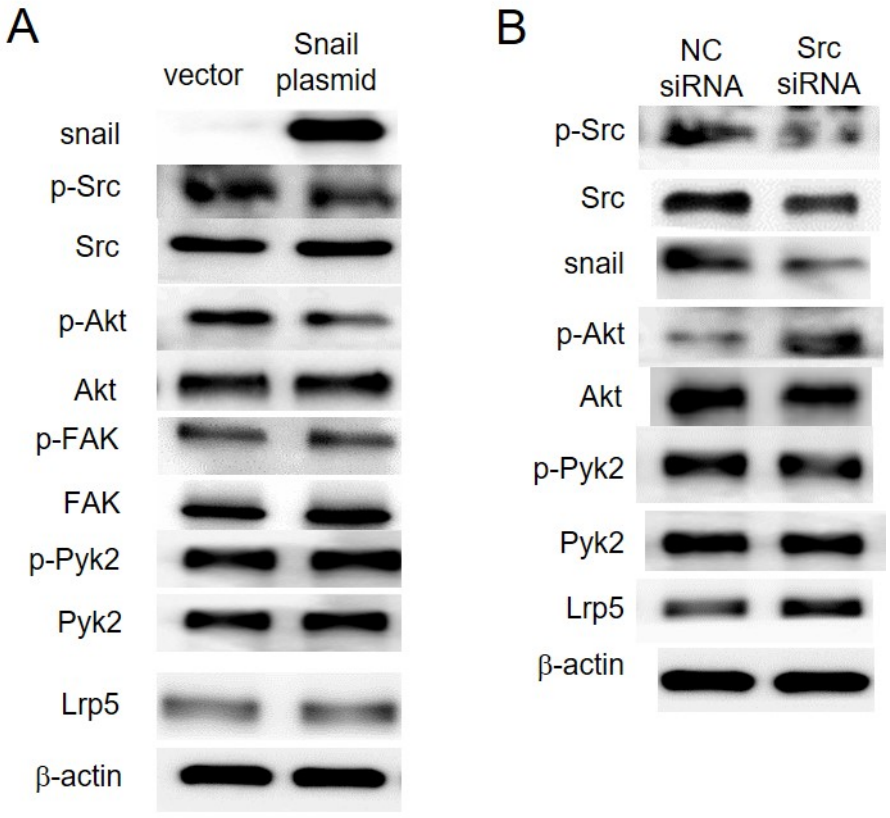

Fig. 3.15.: Src is upstream of Snail and Lrp5 inhibitor. (A) Increased expression of Snail and decreased expression of p-Akt in TMD cells by Snail plasmid. (B) Decreased expression of Src and Snail, and increased expression of p-Akt and Lrp5 by knockdown of Src in TMD cells.

3.6.3 Effect of Src and Snail on TMD Cells Migration

To test our hypothesis and study the relation between Snail and Src expression on breast cancer cells migratory behavior, a 2-dimensional wound healing scratch assay was conducted using Snail plasmid and siRNA specific to Src. As it is shown in Figure

3.16 Snail plasmid promoted migration significantly, and the relative wound area after 24 hour was significantly smaller than the control group ($p<0.05$). Furthermore, the results indicated that silencing Src expression using si-RNA inhibited tumor cells migration. Relative wound area of Src siRNA treated group were 45% larger than the control group ($p<0.01$).

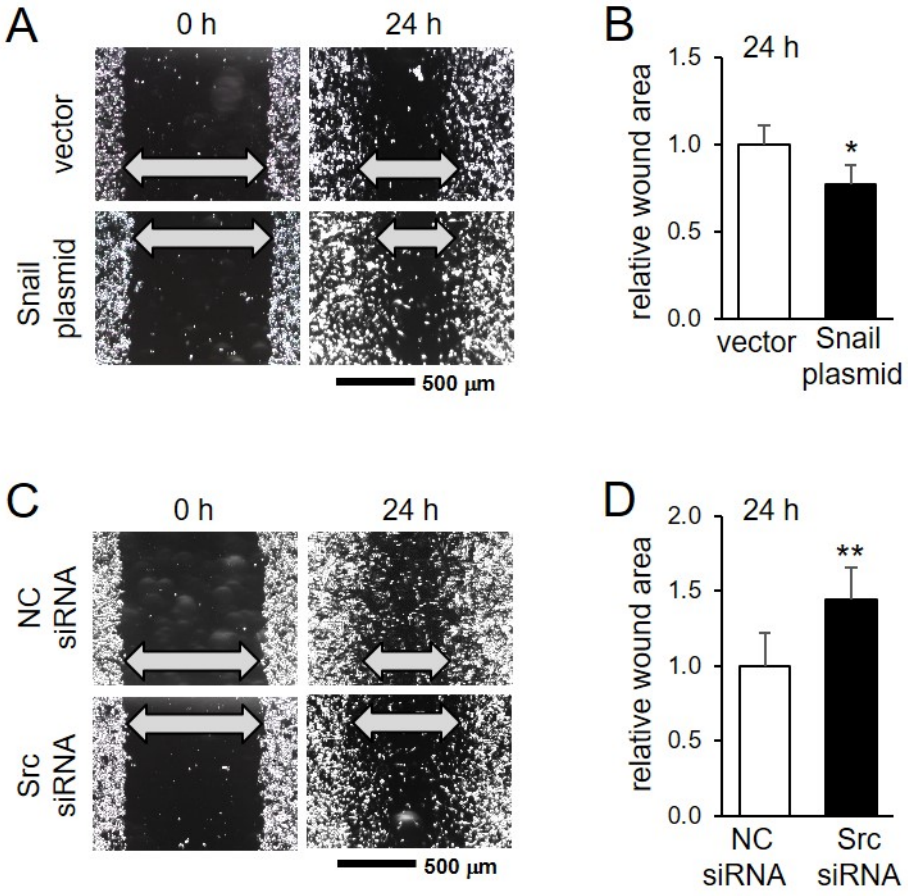

Fig. 3.16.: Effect of Src and Snail on TMD cells migration. (A&B) Higher motility of TMD cells by Snail plasmid transfection. (C&D) Lower motility of TMD cells by Src knockdown.

3.7 Src Activity Screening by FRET

Based on the previous results, the relation and involvement of Src in upregulation of Snail and tumor cells responses was established. To further investigate the Src activity, a Cyto-Src FRET biosensor was used to study the Src cytoplasmic activity in real-time. Figure 3.17 represents the FRET measurements. The results from FRET measurement confirmed that the Src activity is downregulated with A5 CM, while flow treatment prevents MLO-A5 CM downregulation of Src in TMD cells. Collagen was used as an Src suppressor agent and positive control.

3.8 Effect of MLO-A5 CM and FFCM on Tumor-Bone Infusion

A 3-dimensional spheroid fusion assay was used to investigate the effect of MLO-A5 conditioned medium, with and without flow treatment, on the rate and efficacy of tumor-osteocytes spheroids diffusion. As it is shown in Figure 3.18, after 72 hours, cross-sectional area of MLO-A5 CM treated samples was significantly smaller than MLO-A5 FFCM treated ones. Which implies that in the presence of MLO-A5 FFCM tumor cells behave more migratory, and aggressive compared to MLO-A5 CM.

3.9 Effect of Fluid Flow Treatment on MLO-A5 Osteocytes

To investigate how fluid flow treatment changes the conditioned medium efficacy and tumor-osteocytes interactions, osteocytes proteins were harvested directly after the treatment. Subsequently, by western blot analysis, it was illustrated that TGF-β expression was upregulated in MLO-A5 osteocytes which were treated with fluid flow. Furthermore, by using ELISA kit, TGF-β concentration in MLO-A5 CM and FFCM, was measured. As the results in Figure 3.19 show, the relative TGF-β concentration was significantly higher in MLO-A5 FFCM than no-flow treated conditioned medium.

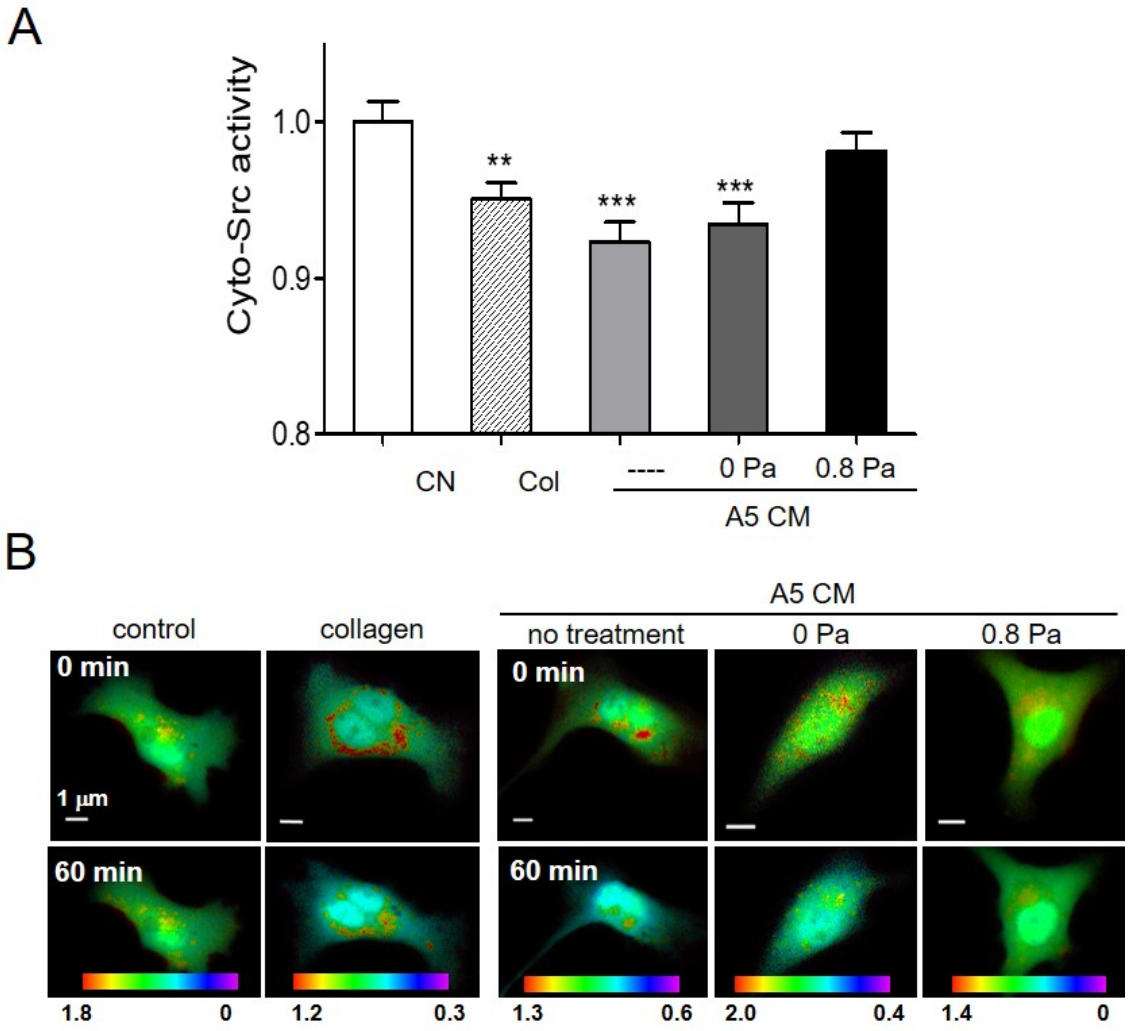

Fig. 3.17.: : Differential dynamics of Cyto-Src activation in TMD cells by collagen, MLO-A5 CM, and FFCM. (A) Src activities in response to the addition of collagen, and presence of MLO-A5 CM, and FFCM. (B) The FRET ratio images and time course of Cyto-Src activities in response to the addition of collagen, and presence of MLO-A5 CM, and FFCM.

3.10 Effect of TGF-β on p-Src and Snail Expression in TMD Cell

As it was mentioned before, cytokines can promote tumor progression and contribute to invasion and migration. Previous results indicated that TGF-β concentra-

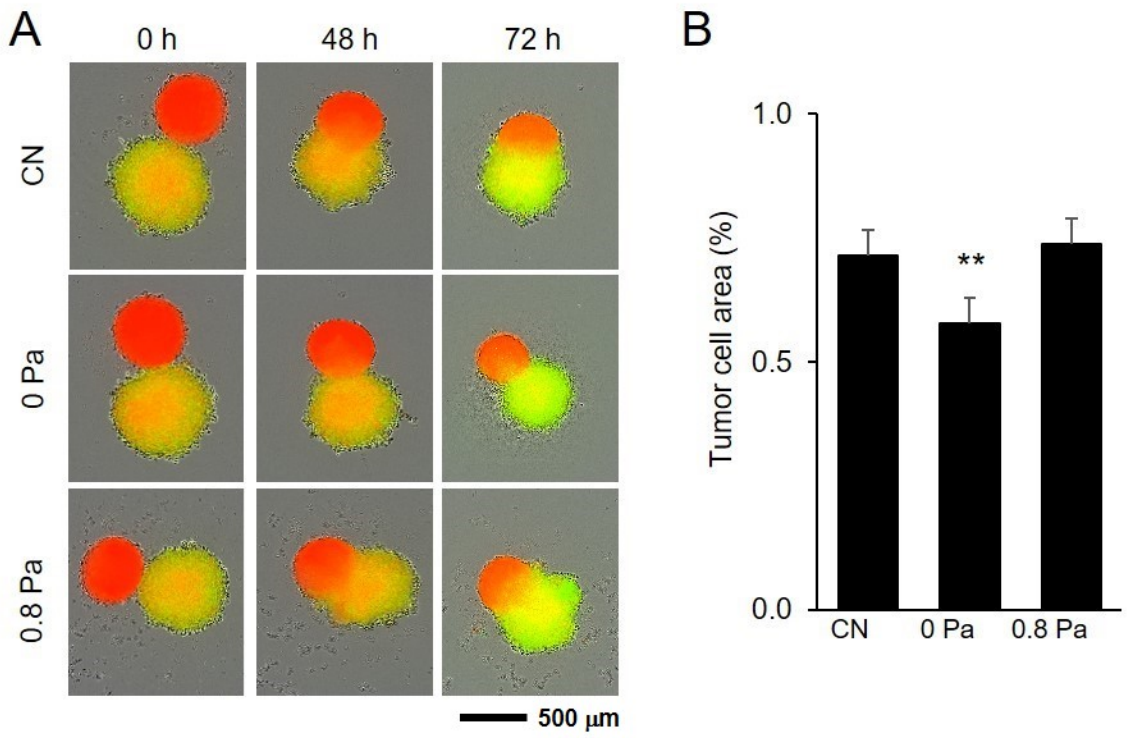

Fig. 3.18.: Effect of MLO-A5 CM and FFCM on tumor-bone diffusion. (A) Higher tumor-bone diffusion rate in the presence of MLO-A5 FFCM than MLO-A5 CM. (B) changes in TMD spheroids cross-sectional area in the presence of MLO-A5 CM and FFCM.

tion is increased due to the flow treatment in MLO-A5 FFCM. To investigate the effect of TGF-β on tumor cells protein expression, 10 and 100 ng/ml of TGF-β1 and TGF-β3 were added to the TMD cells culture medium, separately. As the results in Figure 3.20 show, the Snail expression is upregulated in all cases. The results revealed that p-Src expression did not change with TGF-β1 addition. However, addition of TGF-β3 promoted the p-Src expression in TMD cells in a dose-dependent manner.

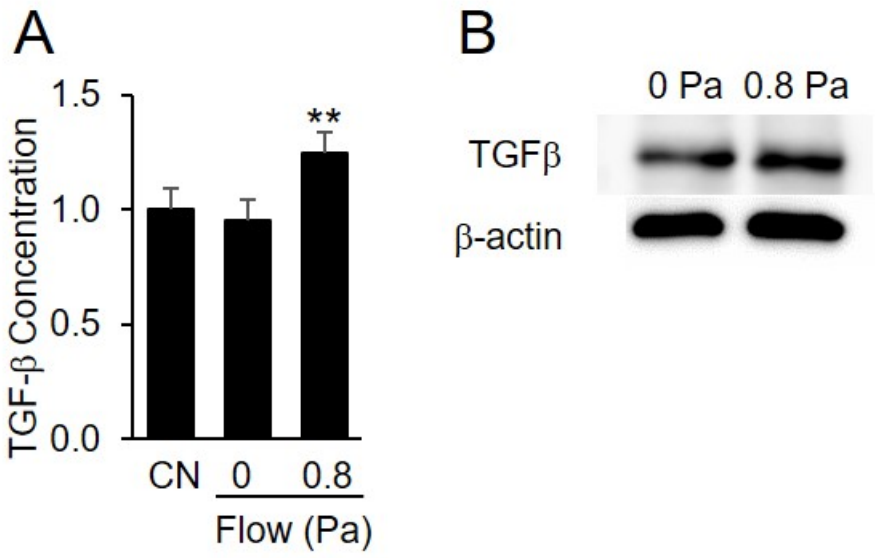

Fig. 3.19.: Effect of fluid flow treatment on MLO-A5 osteocytes. (A) Relative Higher concentration of TGF-β in MLO-A5 FFCM than MLO-A5 CM and control based on ELISA assay. (B) Protein level of TGF-β in MLO-A5 osteocytes with and without fluid flow treatment.

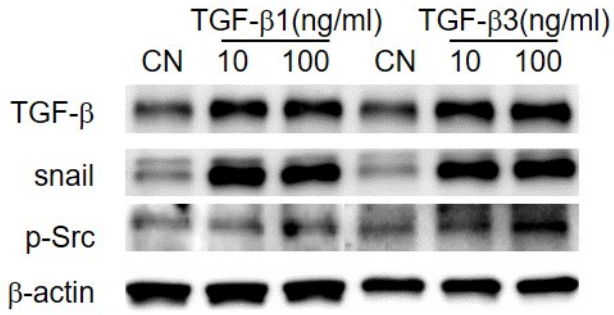

Fig. 3.20.: Effect of TGF-β on p-Src and Snail expression in TMD cells. Protein level of Snail and p-Src in response to the addition of TGF-β1 and TGF-β3 in TMD cells.

3.11 Tibia Loading and Bone Metastasis

3.11.1 Mice Bodyweight

With the beginning of the treatment, the mice body weight was measured every day after loading for three weeks until sacrifice. At the initiation of the tibia loading, the mean body weight for the sham loading mice was 18.29 ± 0.69 gr, and the loading group was 18.25 ± 0.86 gr. As the Figure 3.21 shows, the body weights did not change significantly in either group throughout the study, and the body weights were remained within the expected range based on the age, sex, and condition.

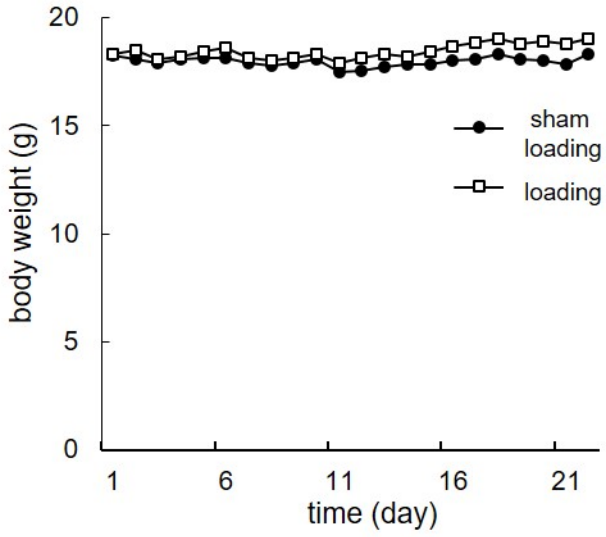

Fig. 3.21.: Mice bodyweight during treatment period.

3.11.2 Bone Phenotype and Mechanical Properties

As it is shown in Figure 3.22, tumor induction in mouse tibia caused significant structural changes in bone. To investigate the changes, μCT and X-ray images were taken from tibia. By using μCT images, the cross-sectional image of proximal regions of the tibia were extracted. The X-ray images suggested that loading mice knee

joint is more fragile than the sham loading group. In addition, loading mice tibia bones showed more smoother shaft than sham loading group. Furthermore, the μCT results revealed the osteoblastic regions are more detectable in sham loading mice. However, these osteoblastic regions were accompanied with architectural deterioration of bone structure and morphological bone degeneration. Also, the cross-sectional images indicated that more discontinuity and osteolysis occured in the loading mice.

As it is shown in Figure 3.23 bending stiffness of the loading mice tibia *ex vivo* was 23% higher than sham loading mice, but not statistically significant (p=0.18). Moreover, axial stiffness was also measured. However, no significant difference were seen between the groups.

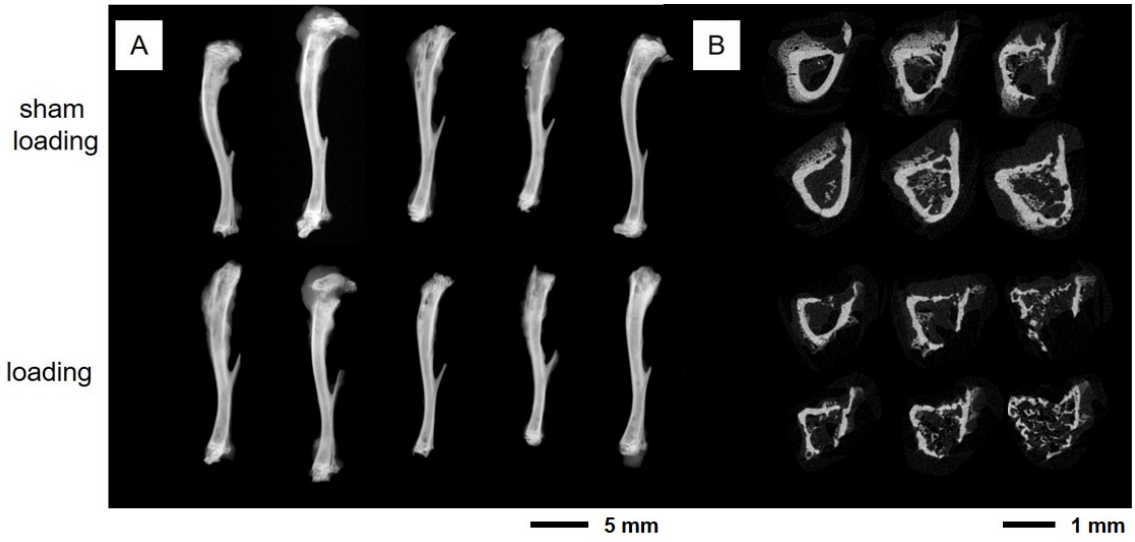

Fig. 3.22.: Effect of tumor induction on bone topography.(A) Representative X-ray images of sham loading and loading tumor induced tibia bones after harvest. (B) Representative cross-sectional μCT images of osteoblastic and osteolytic regions of tibia bone in sham loading and loading mice.

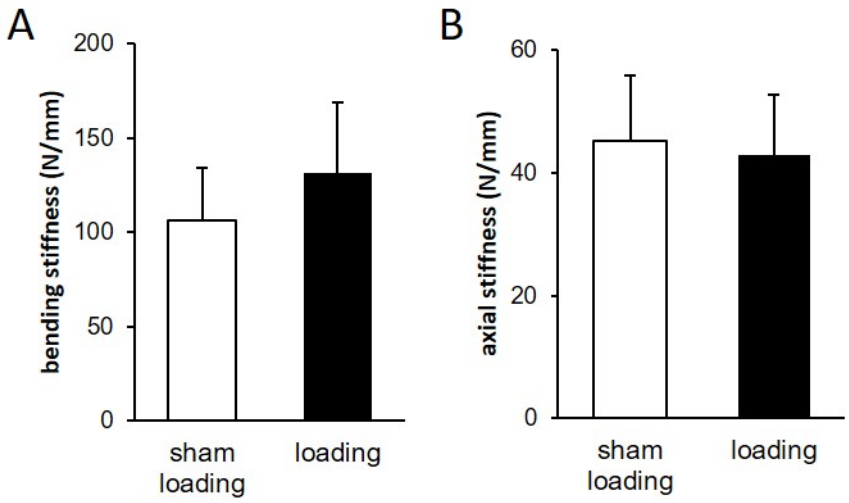

Fig. 3.23.: Tibia mechanical properties (*ex vivo* assesment). (A&B) Two parameters of bone mechanical properties (axial stiffness, and bending stiffness) *ex vivo*.

3.11.3 Tumor-Mediated Bone Degradation and Loading Effect

The results showed that percent bone volume (BV)/tissue volume (TV) of the sham loading was significantly better than the loading mice (p¡0.05). Furthermore, bone mineral density was measured. Even though, no statistically significant differences were seen between the groups, the results trend suggested that sham loading mice tibia bone has higher bone mineral density compared to loading mice. Based on the results, the bone mineral density of the sham loading mice tibia was 6% higher than loading mice tibia (p=0.09). Furthermore, to quantify the bone loss at the knee region, the bone volume was measured. The results showed significant smaller bone volume for loading mice compared to sham loading. Overall, the results trend showed higher bone loss and architectural destruction in loading mice than sham loading.

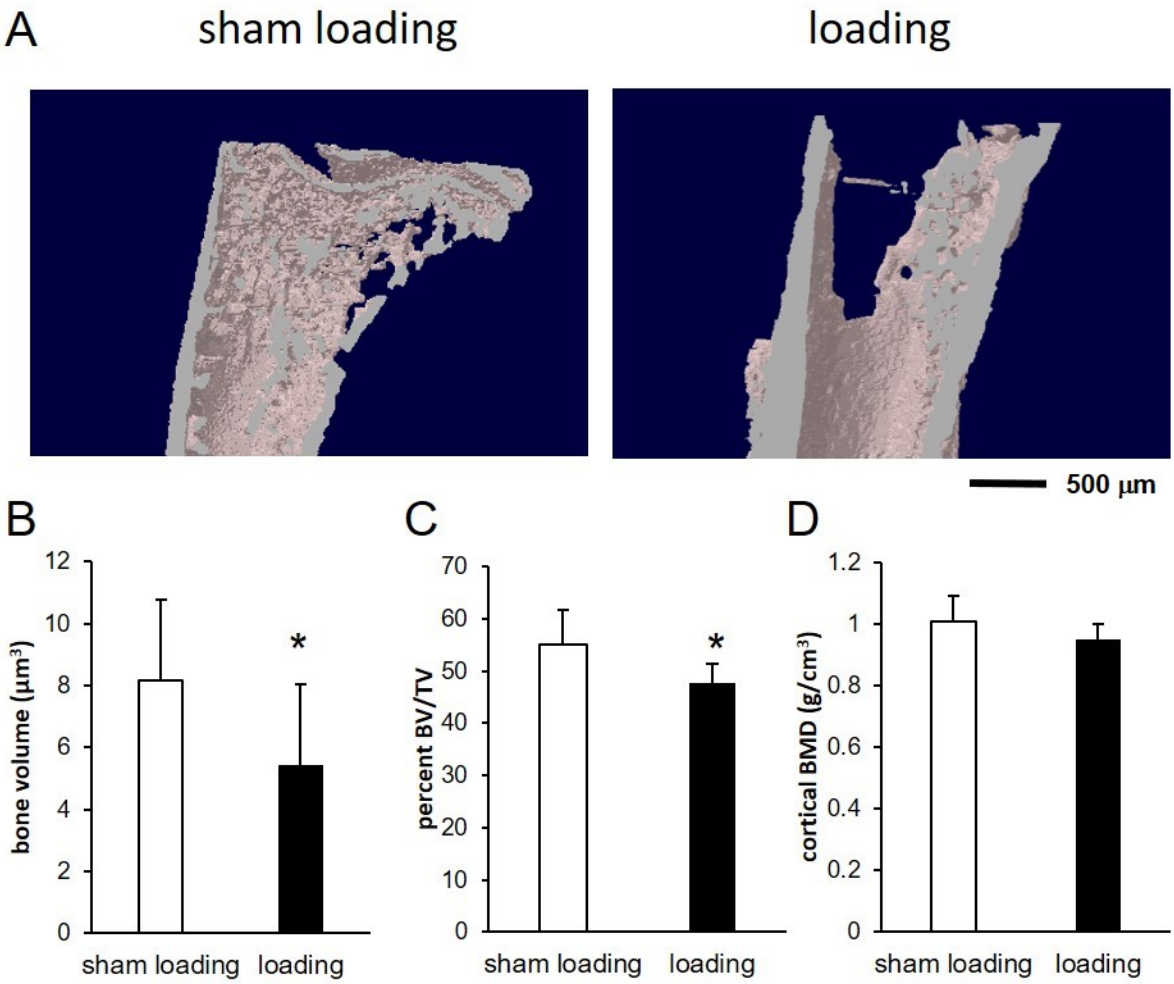

Fig. 3.24.: Bone mass and architecture evaluation by μCT. (AB) Representative 3D reconstructed μCT images of tibia bone and the regions of interest. (B-D) Three tibia bone structural parameters (bone volume, percent BV/TV, cortical BMD) by μCT.

4. DISCUSSION

This thesis presented how FF treatment on osteocytes can change breast cancer cells interaction with bone microenvironment and avert the MET changes in them. Our study confirmed that MLO-A5 conditioned medium could suppress TMD cells migration with downregulation of Src and Snail expression. Moreover, MLO-A5 CM can upregulate p-Akt expression and increase proliferation of breast cancer cells. However, by applying shear stress to osteocytes, the effects of the conditioned medium are reversed. Based on the results, MLO-A5 FFCM upregulated Src and Snail expression, promoted migration, and diminished proliferation. By silencing Src using Si-RNA and overexpressing Snail by plasmid transfection, it was demonstrated that fluid flow could stimulate Src and Snail expressions. Furthermore, FRET measurements revealed that MLO-A5 FFCM increases the Src activity and intra-cellular molecular force in breast cancer cells. In summary, our study suggests that applying oscillating fluid flow shear stress on osteocytes can alter the bone microenvironment and creates an EMT-promoting condition for breast cancer cells.

The mechanical properties of the tumor environment can significantly impact on its progression. For instance, the ECM stiffness can adjust tumor cells and stromal cells proliferation rate and survival [54]. In addition, studies have shown that increased pressure on tumor cells can also increase their growth in metastatic prostate cancer patients [55]. All in all, in most cases direct mechanical stimulation of tumor cells has shown to promote their migratory and invasive behavior [56]. In this study, no direct mechanical stimulation was applied to cancer cells. However, we investigated how mechanical stimulation on osteocytes can affect interactions between migratory breast cancer cells and bone environment. As it was mentioned before, osteocytes receive 0.8-3 Pa shear stress *in vivo* because of the pressure gradients due to compressive forces which stimulate the interstitial fluid through the lacunar-canalicular porosities.

The pressure gradients can change due to the body activity. For the purpose of this study, we used oscillatory fluid flow at 1 Hz with 0.2 and 0.8 Pa, since regular daily activities can create physiologically relevant stress between 0.1 to 1 Pa [39].

Snail is a family of transcription factors which regulate and suppress the expression of E-cadherin, which makes it one of the critical factors in EMT process [57]. EMT is crucial for breast cancer metastasis, cellular migration, invasion, and intravasation. Moreover, recent studies have shown that Snail upregulation can also contribute to metastasis by induction of immune-suppression [58]. In this research, it was demonstrated that MLO-A5 conditioned medium could significantly reduce Snail expression in invasive breast cancer cells. On the contrary, it was shown that MLO-A5 FF treated conditioned medium can prevent this suppression and contribute to cancer cells cellular migration and invasion. Studies have shown that different factors including TGF-β, Notch, Wnt, TNF-α, etc., and cytokines can induce EMT, which in most cases Snail expression has been found as an EMT marker. Snail can reverse tumor suppressor effect of TGF-β and promote tumor progression [7]. In addition, the results from western blot and MTT analysis revealed that MLO-A5 FFCM could downregulate the expression of p-Akt which can lead to inhibition of proliferation in cancer cells. All in all, these changes in cancer cells lead to the development of the notion that MLO-A5 FFCM can inhibit the induction of MET-like responses of MLO-A5 CM, and in the presence of MLO-A5 FFCM cancer cells are in a more invasive stage. It has been suggested that the presence of secretory factors such as collagen, osteonectin, and biglycan are responsible for the MET-like responses of breast cancer cells in the presence of MLO-A5 CM [59]. However, the underlying mechanism of how collagen can induce MET in cancer cells, and how MLO-A5 FFCM can suppress the effect of MLO-A5 CM are not clear. Taken together, while it seems MLO-A5 cells provide a nurturing environment for tumor cells, mechanical interference completely changes these characteristics and prevents the MET induction of MLO-A5 CM.

While it seems that tumor cells are sensitive to the amount of pressure, and the mechanical properties of their microenvironment [60], we observed that the lower

amount of shear stress applied to MLO-A5 osteocytes leads to the same effects as higher amount of shear stress. Thus, it seems that at this order, the osteocytes response is independent of the amount of fluid shear stress. These results raise the possibility that even consistent low-intensity physical activity in breast cancer patients might change the bone metastases process and tumor bone interactions. However, further investigation is needed to understand the pressure dose response of the osteocytes fully. Moreover, only 1-hour time point has been addressed in this study, and more analysis is needed to check the efficacy of other time points and both osteocytes and tumor cells response.

In addition to MDA-MB-231 human breast cancer cell line, our results indicated that MLO-A5 FFCM could induce the same effect on 4T1 cells which are murine breast cancer cell line. This observation shows that while cross-species effect might play a role in cells and conditioned medium interactions, the effect of MLO-A5 FFCM is independent of the type of the cancer cell line. Based on Shengzhi et al. report, MLO-A5 CM can induce the similar MET-like responses in 4T1 cells including Snail downregulation and p-Akt upregulation [61]. In this thesis, we intensively investigated MLO-A5 osteocytes and TMD cells interactions, however, different cell types might show different characteristics. For instance, it has been shown that MLO-Y4 osteocytes (mature osteocytes) conditioned medium, can shrink tumor spheroids more extensively compared to MLO-A5 osteocytes conditioned medium [59]. Moreover, TMD cells seem to show more migratory behavior than BMD cells. Future investigations are needed to illustrate the cell types impact on these interactions and fluid flow effect.

We hypothesized that Wnt signaling could be the critical player of tumor behavioral alterations to MLO-A5 FFCM. The results showed that adding Wnt3a causes tumor spheroid expansion and increase the migration. Moreover, it was shown that Wnt3a could also upregulate Snail expression in breast cancer cells. While, XAV agent as oppose to Wnt3a, caused tumor spheroid shrinkage, decreased cellular migration rate, and downregulated the Snail expression. Thus, it strengthened our notion that

Wnt3a is extensively involved of the effect we was seeing. However, β-catenin and Lrp5 expressions of MLO-A5 CM and MLO-A5 FFCM treated cells showed that Wnt signaling is less likely to be involved in these changes. As it is presented, no significant changes were seen in the expression of β-catenin and p-β-catenin. Moreover, the Lrp5 expression is significantly upregulated by the MLO-A5 FFCM. However, Wnt3a as a Wnt stimulator downregulated Lrp5 expression. In addition, in contrast to the effect of MLO-A5 FFCM, Wnt3a increased the proliferation rate in tumor cells while XAV decreased it. All in all, the data suggested that something other than Wnt signaling is involved in these behavioral alterations.

Src is a non-receptor tyrosine kinase. By silencing Src using Src si-RNA, our study confirmed that Src is upstream of Snail which is crucial for EMT and metastasis promotion [62]. Moreover, the p-FAK expression was changed with p-Src. Furthermore, studies have shown that Src plays a vital role in cancer progression [63]. Src can be activated by cytokine and growth factors. In addition, mechanical stimulation can increase Src activities by ECM-integrin interactions [51]. Since no direct mechanical stimulation was applied to cancer cells, we hypothesized that fluid flow shear stress had changed levels of growth factors or cytokines such as TGFβ, in the conditioned medium. To test this hypothesis, different proteins expressions were studied in osteocytes with and without fluid flow treatment. The results showed that TGF-β expression in osteocytes is upregulated due to flow. However, no significant changes were seen in other proteins expression which could potentially affect the tumor-osteocytes interactions including BMP2, and S100A. The ELISA assay results revealed that TGF-β concentration is higher in MLO-A5 FFCM which confirmed our notion about TGF-β involvement in EMT-like responses of tumor cells. Focal adhesions play a critical role in cellular migration, by interacting with ECM-integrin complexes [64]. Our FRET assay showed that Src activity along with vinculin-based molecular force, which is a protein in focal adhesions, are altered with conditioned medium. These results suggest that mechanical stimulation can change cytokines secretion such as TGF-β in osteocytes which can change the bone microenvironment. Furthermore,

these cytokines can interact with Src associated integrin receptors on tumor cells and change their gene expression profile and prevent MLO-A5 CM MET-like responses.

Lrp5 which is a co-receptor with Lrp6 and Frizzled proteins, is mainly involved in canonical Wnt signaling pathway. However, it roles in tumor progression and metastasis are not clear. Studies have shown that Lrp5 expression suppresses breast tumor metastasis [65]. However, its downregulation in prostate cancer leads to inclined migration, invasion, and MET-like response [66]. In this study, our results revealed that MLO-A5 FFCM, can stimulate Lrp5 expression while MLO-A5 conditioned medium without any treatment leads to downregulation of Lrp5 and induce a MET-like response in breast cancer cells. Furthermore, we showed that silencing Src can cause an increase in Lrp5 expressions, which suggests Src activity prevents Lrp5.

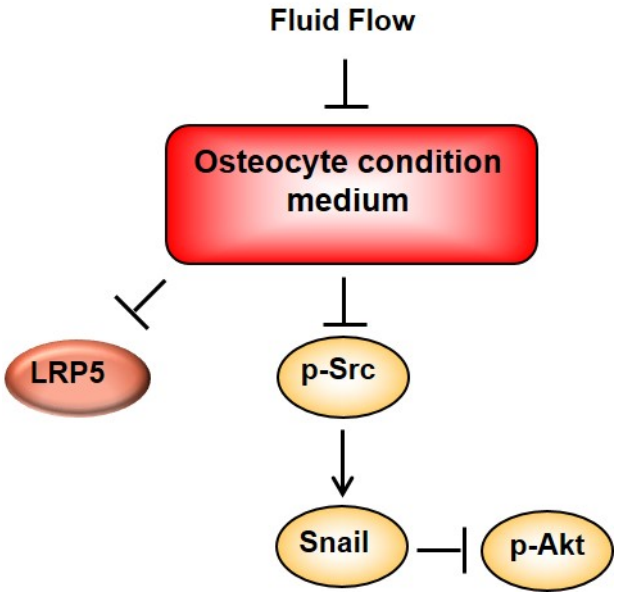

Fig. 4.1.: Effect of fluid flow treatment on osteocyte conditioned medium and tumor cells protein expression. Osteocyte conditioned medium blocked p-Src and LRP5 expression, which lead to Snail downregulation and p-Akt upregulation. However, fluid flow treatment blocked osteocyte conditioned medium effect.

In order to study the effect of mechanical stimulation on physiological and clinical conditions, a study of mouse tibia loading was conducted. Previous studies have

shown that tibia loading can prevent neovascularization and stop tumor progression in loading bones [47]. Our results showed that the mechanical stimulation by tibia compression could potentially alter the tumor-osteocytes interactions. Based on Lynch et al. report tibia loading of SCID mice with MDA-MB-231 tibial injection model, can significantly change the cancer cells behavior in the bone environment causing a significant decrease in tumor formation, and increase in bone formation [47]. However, our results indicated that direct mechanical stimulation can cause damage to the metastasized tibia, and increase the knee joint fragility. Furthermore, our results suggested that these loading conditions might lead to more fractures in bone. It is important to note that, many factors and parameters are involved *in vivo* tumor-bone interactions which are not considered in the *in vitro* model. Moreover, tumor cell line and mouse strain used may effect the conditions and results. In this study, 4T1.2 tumor cell line and BALB/c mouse strain were used. Our animal study results showed both osteoblastic and osteolytic activities in both loading and sham loading mice. Our data analysis suggests that tibia loading might not be beneficial for tumor affected bones, and cause tumor cells to be more aggressive and invasive. However, further investigation is needed to truly understand the effect of mechanical stimulation *in vivo*.

5. CONCLUSIONS

The work in this thesis demonstrates the effect of mechanical stimulation on the bone microenvironment and how it can alter the tumor-osteocytes interactions. Our *in vitro* study using fluid flow shear stress on osteocytes, showed mechanical stimulation between 0.2-0.8 Pa could changes the characteristics of MLO-A5 conditioned medium. While MLO-A5 conditioned medium without treatment can induce MET-like responses in tumor cells, fluid flow treatment can inhibit this effect. As a result, tumor cells were more migratory, and less proliferative. Furthermore, this study showed the crucial role of Src activation in tumor cells in response to changes in osteocytes conditioned medium due to mechanical stimulation. In addition, the role of TGF-β upregulation and its role in response to mechanical stimulation and tumor-osteocytes interactions has been presented. Our *in vivo* study indicated that tibia loading of a tibia bone metastasis mouse model might not be advantageous, and further investigation is needed. It is important to note that the loading conditions are very important, and might change the treatment outcome.

It is important to note that, while the presented results showed the significant effect of mechanical stimulation on tumor-osteocytes interactions, there are a few limitations that need to be considered. Even though we have investigated both mouse and human cancer cells in our study, mouse bone cells and human cancer cells were used as the primary models, and cross-species interactions should be noted. For future studies, deeper investigation in MLO-A5 CM, and FFCM components and other proteins involved using more elaborated assays such as mass spectrometry, can help better understanding the underlying mechanism of fluid flow treatment. Furthermore, a 3D model which can replicate the bone environment might illustrate the role of mechanical stimulation better. Also, further investigation of *in vivo* mechanical

stimulation is needed to show the efficacy of mechanical stimulation in helping bone metastasis patients.

In conclusion, the results from this study suggest that tumor cells and osteocytes conditioned medium interactions completely changes when osteocytes are treated with fluid flow. The results of the tumor-osteocyte signaling can help future studies to understand the underlying mechanism of mechanical stimulation better. Also, it can be used in developing novel therapies and future guidelines of physical therapy to cure or prevent bone metastasis in breast cancer patients.

LIST OF REFERENCES

LIST OF REFERENCES

[1] W. Kozlow and T. A. Guise, "Breast cancer metastasis to bone: Mechanisms of osteolysis and implications for therapy," *Journal of Mammary Gland Biology and Neoplasia*, vol. 10, no. 2, pp. 169–180, 2005.

[2] J. B. Patel, H. N. Appaiah, R. M. Burnett, P. Bhat-Nakshatri, G. Wang, R. Mehta, S. Badve, M. J. Thomson, S. Hammond, P. Steeg, Y. Liu, and H. Nakshatri, "Control of EVI-1 oncogene expression in metastatic breast cancer cells through microRNA miR-22," *Oncogene*, vol. 30, no. 11, pp. 1290–1301, 2011.

[3] B. L. Eckhardt, B. S. Parker, R. K. van Laar, C. M. Restall, A. L. Natoli, M. D. Tavaria, K. L. Stanley, E. K. Sloan, J. M. Moseley, and R. L. Anderson, "Genomic analysis of a spontaneous model of breast cancer metastasis to bone reveals a role for the extracellular matrix." *Molecular cancer research : MCR*, vol. 3, no. 1, pp. 1–13, 2005. [Online]. Available: http://www.ncbi.nlm.nih.gov/pubmed/15671244

[4] M. Mego, S. A. Mani, and M. Cristofanilli, "Molecular mechanisms of metastasis in breast cancer-clinical applications," *Nature Reviews Clinical Oncology*, vol. 7, no. 12, pp. 693–701, 2010.

[5] "The project, Analysis of mirna and mrna associated with, By OpenStax (Page 2/2) — QuizOver.com." [Online]. Available: https://www.quizover.com/course/section/the-project-analysis-of-mirna-and-mrna-associated-with-by-openstax

[6] T. Zhan, N. Rindtorff, and M. Boutros, "Wnt signaling in cancer," *Oncogene*, vol. 36, no. 11, pp. 1461–1473, 2017.

[7] J. Felipe Lima, S. Nofech-Mozes, J. Bayani, and J. Bartlett, "EMT in Breast CarcinomaA Review," *Journal of Clinical Medicine*, vol. 5, no. 7, p. 65, 2016. [Online]. Available: http://www.mdpi.com/2077-0383/5/7/65

[8] L. Zhao, J. W. Shim, T. R. Dodge, A. G. Robling, and H. Yokota, "Inactivation of Lrp5 in osteocytes reduces Young's modulus and responsiveness to the mechanical loading," *Bone*, vol. 54, no. 1, pp. 35–43, 5 2013. [Online]. Available: http://www.ncbi.nlm.nih.gov/pubmed/23356985http://www.pubmedcentral.nih.gov/articlerender.fcgi?artid=PMC3602226http://linkinghub.elsevier.com/retrieve/pii/S8756328213000501

[9] R. Baron and M. Kneissel, "WNT signaling in bone homeostasis and disease: from human mutations to treatments," *Nature Medicine*, vol. 19, no. 2, pp. 179–192, 2 2013. [Online]. Available: http://www.ncbi.nlm.nih.gov/pubmed/23389618http://www.nature.com/articles/nm.3074

[10] G. Farnie and R. B. Clarke, "Mammary stem cells and breast cancer–role of Notch signalling." *Stem cell reviews*, vol. 3, no. 2, pp. 169–75, 6 2007. [Online]. Available: http://www.ncbi.nlm.nih.gov/pubmed/17873349

[11] Y. Li, J. Ma, X. Qian, Q. Wu, J. Xia, L. Miele, F. H. Sarkar, and Z. Wang, "Regulation of EMT by Notch signaling pathway in tumor progression." *Current cancer drug targets*, vol. 13, no. 9, pp. 957–62, 11 2013. [Online]. Available: http://www.ncbi.nlm.nih.gov/pubmed/24168187

[12] C.-W. Li, W. Xia, L. Huo, S.-O. Lim, Y. Wu, J. L. Hsu, C.-H. Chao, H. Yamaguchi, N.-K. Yang, Q. Ding, Y. Wang, Y.-J. Lai, A. M. LaBaff, T.-J. Wu, B.-R. Lin, M.-H. Yang, G. N. Hortobagyi, and M.-C. Hung, "Epithelial-Mesenchymal Transition Induced by TNF- Requires NF-B-Mediated Transcriptional Upregulation of Twist1," *Cancer Research*, vol. 72, no. 5, pp. 1290–1300, 3 2012. [Online]. Available: http://www.ncbi.nlm.nih.gov/pubmed/22253230http://www.pubmedcentral.nih.gov/articlerender.fcgi?artid=PMC3350107http://cancerres.aacrjournals.org/cgi/doi/10.1158/0008-5472.CAN-11-3123

[13] F.-D. Meng, Y. Li, X. Tian, P. Ma, C.-G. Sui, L.-Y. Fu, and Y.-H. Jiang, "Synergistic effects of snail and quercetin on renal cell carcinoma Caki-2 by altering AKT/mTOR/ERK1/2 signaling pathways." *International journal of clinical and experimental pathology*, vol. 8, no. 6, pp. 6157–68, 2015. [Online]. Available: http://www.ncbi.nlm.nih.gov/pubmed/26261493http://www.pubmedcentral.nih.gov/articlerender.fcgi?artid=PMC4525827

[14] S. M. Thomas and J. S. Brugge, "CELLULAR FUNCTIONS REGULATED BY SRC FAMILY KINASES," *Annual Review of Cell and Developmental Biology*, vol. 13, no. 1, pp. 513–609, 11 1997. [Online]. Available: http://www.ncbi.nlm.nih.gov/pubmed/9442882http://www.annualreviews.org/doi/10.1146/annurev.cellbio.13.1.513

[15] D. P. Lesslie, J. M. Summy, N. U. Parikh, F. Fan, J. G. Trevino, T. K. Sawyer, C. A. Metcalf, W. C. Shakespeare, D. J. Hicklin, L. M. Ellis, and G. E. Gallick, "Vascular endothelial growth factor receptor-1 mediates migration of human colorectal carcinoma cells by activation of Src family kinases," *British Journal of Cancer*, vol. 94, no. 11, pp. 1710–1717, 6 2006. [Online]. Available: http://www.ncbi.nlm.nih.gov/pubmed/16685275http://www.pubmedcentral.nih.gov/articlerender.fcgi?artid=PMC2361330http://www.nature.com/articles/6603143

[16] M. Sekharam, A. Nasir, H. E. Kaiser, and D. Coppola, "Insulin-like growth factor 1 receptor activates c-SRC and modifies transformation and motility of colon cancer in vitro." *Anticancer research*, vol. 23, no. 2B, pp. 1517–24. [Online]. Available: http://www.ncbi.nlm.nih.gov/pubmed/12820418

[17] F. Saad and A. Lipton, "SRC kinase inhibition: Targeting bone metastases and tumor growth in prostate and breast cancer," *Cancer Treatment Reviews*, vol. 36, no. 2, pp. 177–184, 2010.

[18] R. Cailleau, M. Olive, and Q. V. Cruciger, "Long-term human breast carcinoma cell lines of metastatic origin: preliminary characterization." *In vitro*, vol. 14, no. 11, pp. 911–915, 11 1978.

[19] Y.-X. Cui, B. A. J. Evans, and W. G. Jiang, "New Roles of Osteocytes in Proliferation, Migration and Invasion of Breast and Prostate Cancer Cells." *Anticancer research*, vol. 36, no. 3, pp. 1193–201, 3 2016. [Online]. Available: http://www.ncbi.nlm.nih.gov/pubmed/26977015

[20] E. Mackie, Y. Ahmed, L. Tatarczuch, K.-S. Chen, and M. Mirams, "Endochondral ossification: How cartilage is converted into bone in the developing skeleton," *The International Journal of Biochemistry & Cell Biology*, vol. 40, no. 1, pp. 46–62, 1 2008. [Online]. Available: https://www.sciencedirect.com/science/article/pii/S135727250700204X?via%3Dihub

[21] E. F. Eriksen, "Cellular mechanisms of bone remodeling," *Reviews in Endocrine and Metabolic Disorders*, vol. 11, no. 4, pp. 219–227, 12 2010. [Online]. Available: http://link.springer.com/10.1007/s11154-010-9153-1

[22] S. Khosla, "Minireview: The OPG/RANKL/RANK System," *Endocrinology*, vol. 142, no. 12, pp. 5050–5055, 12 2001. [Online]. Available: https://academic.oup.com/endo/article-lookup/doi/10.1210/endo.142.12.8536

[23] T. Komori, H. Yagi, S. Nomura, A. Yamaguchi, K. Sasaki, K. Deguchi, Y. Shimizu, R. Bronson, Y.-H. Gao, M. Inada, M. Sato, R. Okamoto, Y. Kitamura, S. Yoshiki, and T. Kishimoto, "Targeted Disruption of Cbfa1 Results in a Complete Lack of Bone Formation owing to Maturational Arrest of Osteoblasts," *Cell*, vol. 89, no. 5, pp. 755–764, 5 1997. [Online]. Available: http://linkinghub.elsevier.com/retrieve/pii/S0092867400802585

[24] L. Qin, P. Qiu, L. Wang, X. Li, J. T. Swarthout, P. Soteropoulos, P. Tolias, and N. C. Partridge, "Gene expression profiles and transcription factors involved in parathyroid hormone signaling in osteoblasts revealed by microarray and bioinformatics." *The Journal of biological chemistry*, vol. 278, no. 22, pp. 19 723–31, 5 2003. [Online]. Available: http://www.ncbi.nlm.nih.gov/pubmed/12644456

[25] L. Bonewald, "Osteocytes as multifunctional cells." *Journal of musculoskeletal & neuronal interactions*, vol. 6, no. 4, pp. 331–3, 2006. [Online]. Available: http://www.ncbi.nlm.nih.gov/pubmed/17185811http://www.pubmedcentral.nih.gov/articlerender.fcgi?artid=PMC1796957

[26] A. F. Stewart, "Editorial Hyperparathyroidism, Humoral Hypercalcemia of Malignancy, and the Anabolic Actions of Parathyroid Hormone and Parathyroid HormoneRelated Protein on the Skeleton." [Online]. Available: https://onlinelibrary.wiley.com/doi/pdf/10.1359/jbmr.2002.17.5.758

[27] Y.-c. Chen, D. M. Sosnoski, and A. M. Mastro, "Breast cancer metastasis to the bone : mechanisms of bone loss," 2010.

[28] T. A. Guise, "Parathyroid hormone-related protein and bone metastases." *Cancer*, vol. 80, no. 8 Suppl, pp. 1572–80, 10 1997. [Online]. Available: http://www.ncbi.nlm.nih.gov/pubmed/9362424

[29] S. Corisdeo, M. Gyda, M. Zaidi, B. S. Moonga, and B. R. Troen, "New Insights into the Regulation of Cathepsin K Gene Expression by Osteoprotegerin Ligand," *Biochemical and Biophysical Research Communications*, vol. 285, no. 2, pp. 335–339, 7 2001. [Online]. Available: https://www.sciencedirect.com/science/article/pii/S0006291X01951277

[30] Y. Kang, P. M. Siegel, W. Shu, M. Drobnjak, S. M. Kakonen, C. Cordón-Cardo, T. A. Guise, and J. Massagué, "A multigenic program mediating breast cancer metastasis to bone," *Cancer Cell*, vol. 3, no. 6, pp. 537–549, 6 2003. [Online]. Available: http://linkinghub.elsevier.com/retrieve/pii/S1535610803001326

[31] Y.-X. Cui, B. A. J. Evans, and W. G. Jiang, "New Roles of Osteocytes in Proliferation, Migration and Invasion of Breast and Prostate Cancer Cells." *Anticancer research*, vol. 36, no. 3, pp. 1193–201, 2016. [Online]. Available: http://www.ncbi.nlm.nih.gov/pubmed/26977015

[32] J. L. Pathak, N. Bravenboer, F. P. Luyten, P. Verschueren, W. F. Lems, J. Klein-Nulend, and A. D. Bakker, "Mechanical loading reduces inflammation-induced human osteocyte-to-osteoclast communication." *Calcified tissue international*, vol. 97, no. 2, pp. 169–78, 8 2015. [Online]. Available: http://www.ncbi.nlm.nih.gov/pubmed/25967362http://www.pubmedcentral.nih.gov/articlerender.fcgi?artid=PMC4491366

[33] R. J. van'T Hof and S. H. Ralston, "Nitric oxide and bone," *Immunology*, vol. 103, no. 3, pp. 255–261, 7 2001. [Online]. Available: http://doi.wiley.com/10.1046/j.1365-2567.2001.01261.x

[34] A. M. Simon, M. B. Manigrasso, and J. P. O'Connor, "Cyclo-Oxygenase 2 Function Is Essential for Bone Fracture Healing," *Journal of Bone and Mineral Research*, vol. 17, no. 6, pp. 963–976, 6 2002. [Online]. Available: http://doi.wiley.com/10.1359/jbmr.2002.17.6.963

[35] Y. H. V. Ma, C. Lam, S. Dalmia, P. Gao, J. Young, K. Middleton, C. Liu, H. Xu, and L. You, "Mechanical regulation of breast cancer migration and apoptosis via direct and indirect osteocyte signaling," *Journal of Cellular Biochemistry*, no. January, pp. 1–11, 2018.

[36] A. Chen, L. Wang, S. Liu, Y. Wang, Y. Liu, M. Wang, H. Nakshatri, B. Y. Li, and H. Yokota, "Attraction and Compaction of Migratory Breast Cancer Cells by Bone Matrix Proteins through Tumor-Osteocyte Interactions," *Scientific Reports*, vol. 8, no. 1, pp. 1–13, 2018. [Online]. Available: http://dx.doi.org/10.1038/s41598-018-23833-1

[37] K. Sakai, M. Mohtai, and Y. Iwamoto, "Fluid shear stress increases transforming growth factor beta 1 expression in human osteoblast-like cells: modulation by cation channel blockades," *Calcif Tissue Int*, vol. 63, no. 6, pp. 515–520, 1998. [Online]. Available: http://www.ncbi.nlm.nih.gov/entrez/query.fcgi?cmd=Retrieve&db=PubMed&dopt=Citation&list_uids=9817947

[38] L. V. Harter, K. A. Hruska, and R. L. Duncan, "Human osteoblast-like cells respond to mechanical strain with increased bone matrix protein production independent of hormonal regulation," *Endocrinology*, vol. 136, no. 2, pp. 528–535, 2 1995. [Online]. Available: https://academic.oup.com/endo/article-lookup/doi/10.1210/en.136.2.528

[39] S. Weinbaum, S. C. Cowin, and Y. Zeng, "A model for the excitation of osteocytes by mechanical loading-induced bone fluid shear stresses." *Journal of biomechanics*, vol. 27, no. 3, pp. 339–60, 3 1994. [Online]. Available: http://www.ncbi.nlm.nih.gov/pubmed/8051194

[40] A. W. Orr, B. P. Helmke, B. R. Blackman, and M. A. Schwartz, "Mechanisms of mechanotransduction," *Developmental Cell*, vol. 10, no. 1, pp. 11–20, 2006.

[41] E. H. Burger and J. Klein-Nulend, "Mechanotransduction in bone–role of the lacuno-canalicular network." *FASEB journal : official publication of the Federation of American Societies for Experimental Biology*, vol. 13 Suppl, pp. 101–12, 1999. [Online]. Available: http://www.ncbi.nlm.nih.gov/pubmed/10352151

[42] L. G. Raisz, "Physiology and pathophysiology of bone remodeling." *Clinical chemistry*, vol. 45, no. 8 Pt 2, pp. 1353–8, 8 1999. [Online]. Available: http://www.ncbi.nlm.nih.gov/pubmed/10430818

[43] F. Weyts, Y.-S. Li, J. van Leeuwen, H. Weinans, and S. Chien, "ERK activation and ?v?3 integrin signaling through Shc recruitment in response to mechanical stimulation in human osteoblasts," *Journal of Cellular Biochemistry*, vol. 87, no. 1, pp. 85–92, 2002. [Online]. Available: http://www.ncbi.nlm.nih.gov/pubmed/12210725http://doi.wiley.com/10.1002/jcb.10278

[44] S. M. Norvell, M. Alvarez, J. P. Bidwell, and F. M. Pavalko, "Fluid shear stress induces β-catenin signaling in osteoblasts," *Calcified Tissue International*, vol. 75, no. 5, pp. 396–404, 2004.

[45] R. L. Duncan and K. A. Hruska, "Chronic, intermittent loading alters mechanosensitive channel characteristics in osteoblast-like cells." *The American journal of physiology*, vol. 267, no. 6 Pt 2, pp. 909–16, 12 1994. [Online]. Available: http://www.ncbi.nlm.nih.gov/pubmed/7528987

[46] R. L. Duncan, N. Kizer, E. L. Barry, P. A. Friedman, and K. A. Hruska, "Antisense oligodeoxynucleotide inhibition of a swelling-activated cation channel in osteoblast-like osteosarcoma cells." *Proceedings of the National Academy of Sciences of the United States of America*, vol. 93, no. 5, pp. 1864–9, 3 1996. [Online]. Available: http://www.ncbi.nlm.nih.gov/pubmed/8700850http://www.pubmedcentral.nih.gov/articlerender.fcgi?artid=PMC39873

[47] M. E. Lynch, D. Brooks, S. Mohanan, M. J. Lee, P. Polamraju, K. Dent, L. J. Bonassar, M. C. Van Der Meulen, and C. Fischbach, "In vivo tibial compression decreases osteolysis and tumor formation in a human metastatic breast cancer model," *Journal of Bone and Mineral Research*, vol. 28, no. 11, pp. 2357–2367, 2013.

[48] L. Vico, P. Collet, A. Guignandon, M. H. Lafage-Proust, T. Thomas, M. Rehaillia, and C. Alexandre, "Effects of long-term microgravity exposure on cancellous and cortical weight-bearing bones of cosmonauts." *Lancet (London, England)*, vol. 355, no. 9215, pp. 1607–11, 5 2000. [Online]. Available: http://www.ncbi.nlm.nih.gov/pubmed/10821365

[49] D. T. Villareal, K. Steger-May, K. B. Schechtman, K. E. Yarasheski, M. Brown, D. R. Sinacore, and E. F. Binder, "Effects of exercise training on bone mineral density in frail older women and men: a randomised controlled trial," *Age and Ageing*, vol. 33, no. 3, pp. 309–312, 5 2004. [Online]. Available: http://www.ncbi.nlm.nih.gov/pubmed/15082440https://academic.oup.com/ageing/article-lookup/doi/10.1093/ageing/afh044

[50] J. W. M. Chow, A. J. Wilson, T. J. Chambers, and S. W. Fox, "Mechanical Loading Stimulates Bone Formation by Reactivation of Bone Lining Cells in 13-Week-Old Rats," *Journal of Bone and Mineral Research*, vol. 13, no. 11, pp. 1760–1767, 11 1998. [Online]. Available: http://doi.wiley.com/10.1359/jbmr.1998.13.11.1760

[51] Q. Wan, W. Xu, J. L. Yan, H. Yokota, and S. Na, "Distinctive subcellular inhibition of cytokine-induced Src by salubrinal and fluid flow," *PLoS ONE*, vol. 9, no. 8, pp. 3–11, 2014.

[52] L. B. Meakin, J. S. Price, and L. E. Lanyon, "The Contribution of Experimental in vivo Models to Understanding the Mechanisms of Adaptation to Mechanical Loading in Bone." *Frontiers in endocrinology*, vol. 5, p. 154, 2014. [Online]. Available: http://www.ncbi.nlm.nih.gov/pubmed/25324829http://www.pubmedcentral.nih.gov/articlerender.fcgi?artid=PMC4181237

[53] X. Bi, J. A. Sterling, A. R. Merkel, D. S. Perrien, J. S. Nyman, and A. Mahadevan-Jansen, "Prostate cancer metastases alter bone mineral and matrix composition independent of effects on bone architecture in mice A quantitative study using microCT and Raman spectroscopy," *Bone*, vol. 56, no. 2, pp. 454–460, 10 2013. [Online]. Available: http://www.ncbi.nlm.nih.gov/pubmed/23867219http://www.pubmedcentral.nih.gov/articlerender.fcgi?artid=PMC3799839http://linkinghub.elsevier.com/retrieve/pii/S8756328213002664

[54] H. J. Lee, M. F. Diaz, K. M. Price, J. A. Ozuna, S. Zhang, E. M. Sevick-Muraca, J. P. Hagan, and P. L. Wenzel, "Fluid shear stress activates YAP1 to promote cancer cell motility," *Nature Communications*, vol. 8, p. 14122, 1 2017. [Online]. Available: http://www.nature.com/doifinder/10.1038/ncomms14122

[55] J. M. Tse, G. Cheng, J. A. Tyrrell, S. A. Wilcox-Adelman, Y. Boucher, R. K. Jain, and L. L. Munn, "Mechanical compression drives cancer cells toward invasive phenotype," *Proceedings of the National Academy of Sciences*, vol. 109, no. 3, pp. 911–916, 1 2012. [Online]. Available: http://www.ncbi.nlm.nih.gov/pubmed/22203958http://www.pubmedcentral.nih.gov/articlerender.fcgi?artid=PMC3271885http://www.pnas.org/cgi/doi/10.1073/pnas.1118910109

[56] D. Wirtz, K. Konstantopoulos, and P. C. Searson, "The physics of cancer: the role of physical interactions and mechanical forces in metastasis," *Nature Reviews Cancer*, vol. 11, no. 7, pp. 512–522, 7 2011. [Online]. Available: http://www.nature.com/articles/nrc3080

[57] S. J. Grille, A. Bellacosa, J. Upson, A. J. Klein-Szanto, F. van Roy, W. Lee-Kwon, M. Donowitz, P. N. Tsichlis, and L. Larue, "The protein kinase Akt induces epithelial mesenchymal transition and promotes enhanced motility and invasiveness of squamous cell carcinoma lines." *Cancer research*, vol. 63, no. 9, pp. 2172–8, 5 2003. [Online]. Available: http://www.ncbi.nlm.nih.gov/pubmed/12727836

[58] Y. Wang, J. Shi, K. Chai, X. Ying, and B. P. Zhou, "The Role of Snail in EMT and Tumorigenesis." [Online]. Available: http://www.ingentaconnect.com/content/ben/ccdt/2013/00000013/00000009/art00008

[59] A. Chen, L. Wang, B.-Y. Li, J. Sherman, J. E. Ryu, K. Hamamura, Y. Liu, H. Nakshatri, and H. Yokota, "Reduction in Migratory Phenotype in a Metastasized Breast Cancer Cell Line via Downregulation of S100A4 and GRM3," *Scientific Reports*, vol. 7, no. 1, p. 3459, 2017. [Online]. Available: http://www.nature.com/articles/s41598-017-03811-9

[60] A. B. Ariffin, P. F. Forde, S. Jahangeer, D. M. Soden, and J. Hinchion, "Releasing Pressure in Tumors: What Do We Know So Far and Where Do We Go from Here? A Review," *Cancer Research*, vol. 74, no. 10, pp. 2655–2662, 5 2014. [Online]. Available: http://www.ncbi.nlm.nih.gov/pubmed/24778418http://cancerres.aacrjournals.org/cgi/doi/10.1158/0008-5472.CAN-13-3696

[61] S. Liu, Y. Fan, A. Chen, A. Jalali, K. Minami, K. Ogawa, H. Nakshatri, B.-Y. Li, and H. Yokota, "Osteocyte-Driven Downregulation of Snail Restrains Effects of Drd2 Inhibitors on Mammary Tumor Cells." *Cancer research*, p. canres.0056.2018, 5 2018. [Online]. Available: http://www.ncbi.nlm.nih.gov/pubmed/29769195

[62] T. Tomono, K. Yano, and T. Ogihara, "Snail-Induced Epithelial-to-Mesenchymal Transition Enhances P-gp-Mediated Multidrug Resistance in HCC827 Cells." *Journal of pharmaceutical sciences*, vol. 106, no. 9, pp. 2642–2649, 9 2017. [Online]. Available: http://www.ncbi.nlm.nih.gov/pubmed/28322937

[63] X. H. F. Zhang, Q. Wang, W. Gerald, C. A. Hudis, L. Norton, M. Smid, J. A. Foekens, and J. Massagué, "Latent Bone Metastasis in Breast Cancer Tied to Src-Dependent Survival Signals," *Cancer Cell*, vol. 16, no. 1, pp. 67–78, 2009.

[64] H. Yoon, J. P. Dehart, J. M. Murphy, and S.-T. S. Lim, "Understanding the roles of FAK in cancer: inhibitors, genetic models, and new insights." *The journal of histochemistry and cytochemistry : official journal of the Histochemistry Society*, vol. 63, no. 2, pp. 114–28, 2015. [Online]. Available: http://www.ncbi.nlm.nih.gov/pubmed/25380750http://www.pubmedcentral.nih.gov/articlerender.fcgi?artid=PMC4305513

[65] D.-n. Ren, J. Chen, Z. Li, H. Yan, Y. Yin, D. Wo, J. Zhang, L. Ao, B. Chen, T. K. Ito, Y. Chen, Z. Liu, Y. Li, J. Yang, X. Lu, Y. Peng, L. Pan, Y. Zhao, S. Liu, and W. Zhu, "LRP5/6 directly bind to Frizzled and prevent Frizzled-regulated tumour metastasis," *Nature Communications*, vol. 6, no. 1, p. 6906, 12 2015. [Online]. Available: http://www.ncbi.nlm.nih.gov/pubmed/25902418http://www.nature.com/articles/ncomms7906

[66] S. A. Rabbani, A. Arakelian, and R. Farookhi, "LRP5 knockdown: effect on prostate cancer invasion growth and skeletal metastasis ¡i¿in vitro¡/i¿ and ¡i¿in vivo¡/i¿," *Cancer Medicine*, vol. 2, no. 5, pp. n/a–n/a, 9 2013. [Online]. Available: http://www.ncbi.nlm.nih.gov/pubmed/24403228http://www.pubmedcentral.nih.gov/articlerender.fcgi?artid=PMC3892794http://doi.wiley.com/10.1002/cam4.111

APPENDIX

APPENDIX

MATLAB script for stiffness measurement:

```
clear;
clc;

d=dir('C:\Users\Aydin\Documents\MATLAB\*.csv');



n9=length(d)
for ni=1:n9
M=csvread(d(ni).name,54,0,[54 0 14050 5]);
n1=length(M(:,3));
%plot(M(:,2),M(:,5))
o=0;
for i=2:n1
    if M(i,3)==0
        o=o+1;
        v(o)=i;
    end
end
v=[1,v,n1];

n2=length(v);
```

```
o1=0;
for i=1:n2-1
    x=M(v(i):v(i+1),2);
    y=M(v(i):v(i+1),5);
    [fmin, imin]=min(y);
    yl=length(y);
    y(imin:yl)=[];
    x(imin:yl)=[];
    [fmax, imax]=max(y);
    y(1:imax)=[];
    x(1:imax)=[];
    xlength=length(x);
    z=[];
    if xlength>0
    [D1, II1] = min(abs(M(:,2)-x(1)));
    [D2, II2] = min(abs(M(:,2)-x(xlength)));
    z=M(II1:II2,6);
    end

    minf=min(y);
    maxf=max(y);
    dd=minf-maxf;
    f1=dd/4+maxf;
    f2=dd/2+maxf;

    if xlength>0
    [DD1, III1] = min(abs(y-f1));
    [DD2, III2] = min(abs(y-f2));
    y1=y(III1:III2);
```

```
    z1=z(III1:III2);
    end


    if length(z)>0
    o1=o1+1;
    sti=polyfit(z1,y1,1);
    stif(o1)=sti(:,1);
    end

%      figure(i)
%      plot(z,y);

end
final(:,ni)=stif;
csvwrite('stiffness.csv',final);
end
```